Do Vision-Language Models Represent Space and How? Evaluating Spatial Frame of Reference under Ambiguities

Zheyuan Zhang[1]* **Fengyuan Hu**[1]* **Jayjun Lee**[1]*
Freda Shi[2,3] **Parisa Kordjamshidi**[4] **Joyce Chai**[1] **Ziqiao Ma**[1]
[1]University of Michigan [2]University of Waterloo [3]Vector Institute [4]Michigan State University
https://spatial-comfort.github.io/

Abstract

Spatial expressions in situated communication can be ambiguous, as their meanings vary depending on the frames of reference (FoR) adopted by speakers and listeners. While spatial language understanding and reasoning by vision-language models (VLMs) have gained increasing attention, potential ambiguities in these models are still under-explored. To address this issue, we present the COnsistent Multilingual Frame Of Reference Test (COMFORT), an evaluation protocol to systematically assess the spatial reasoning capabilities of VLMs. We evaluate nine state-of-the-art VLMs using COMFORT. Despite showing some alignment with English conventions in resolving ambiguities, our experiments reveal significant shortcomings of VLMs: notably, the models (1) exhibit poor robustness and consistency, (2) lack the flexibility to accommodate multiple FoRs, and (3) fail to adhere to language-specific or culture-specific conventions in cross-lingual tests, as English tends to dominate other languages. With a growing effort to align vision-language models with human cognitive intuitions, we call for more attention to the ambiguous nature and cross-cultural diversity of spatial reasoning.

1 Introduction

The recent success of large language models has sparked breakthroughs in multi-modalities, leading to the development of many vision-language models (VLMs; Chen et al., 2023c; OpenAI, 2024; Reid et al., 2024, *inter alia*). With some benchmarks developed to evaluate the downstream performance of these models (Liu et al., 2023c; Yue et al., 2024), there has been growing excitement around evaluations and analyses inspired by human cognitive capabilities such as referential grounding (Ma et al., 2023a), compositional reasoning (Ma et al., 2023c), visual illusions (Zhang et al., 2023; Guan et al., 2024), and theory of mind (Jin et al., 2024). One direction among them that captures significant attention is spatial language understanding and reasoning, leading to several benchmarks (Mirzaee et al., 2021; Mirzaee & Kordjamshidi, 2022; Kamath et al., 2023; Liu et al., 2023a) and enhanced models (Chen et al., 2024a; Cheng et al., 2024; Premsri & Kordjamshidi, 2025).

Indeed, spatial cognition is a crucial part of human cognitive capability developed in early ages (Tommasi & Laeng, 2012; Vasilyeva & Lourenco, 2012). Language is closely intertwined with spatial cognition, with each contributing to the acquisition of the other (Hayward & Tarr, 1995; Regier & Carlson, 2001; Pyers et al., 2010; Pruden et al., 2011; Gentner et al., 2013). While spatial language and non-linguistic spatial representations in memory are closely correlated and share foundational properties, they are, to some extent, divergent—spatial conventions are not consistently preserved across different languages or tasks, and humans demonstrate flexibility in using multiple coordinate systems for both non-linguistic reasoning and linguistic expressions (Munnich et al., 2001; Shusterman & Li, 2016). Thus, spatial language is inherently ambiguous.

In situated communication, even a simple spatial expression like "the basketball to the right of the car" may have multiple interpretations. People may use different *frames of reference* (FoR; Levinson, 1996; Frank, 1998, *inter alia*) to resolve ambiguity about the underlying coordinate system, as illustrated in Figure 1a. The diversity of conventions across languages and cultures further

---

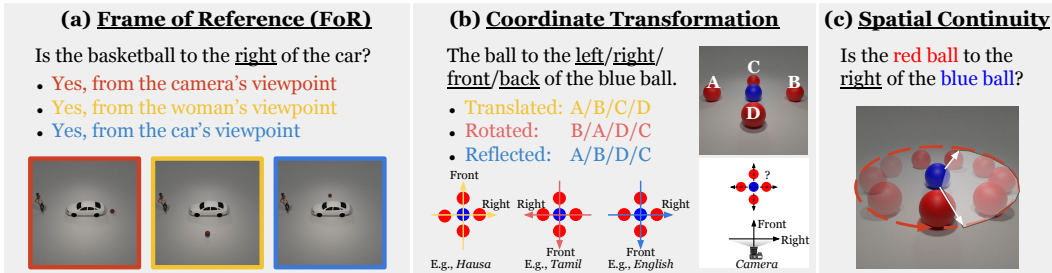*Authors contributed equally to this work.

(a) Frame of Reference (FoR)

Is the basketball to the <u>right</u> of the car?
- Yes, from the camera's viewpoint
- Yes, from the woman's viewpoint
- Yes, from the car's viewpoint

(b) Coordinate Transformation

The ball to the <u>left/right/front/back</u> of the blue ball.
- Translated: A/B/C/D
- Rotated: B/A/D/C
- Reflected: A/B/D/C

E.g., *Hausa* E.g., *Tamil* E.g., *English*

(c) Spatial Continuity

Is the red ball to the <u>right</u> of the blue ball?

Figure 1: In situated communication, spatial language understanding and reasoning are often ambiguous, leading to varying interpretations among people from different cultural backgrounds. Specifically: (a) different frames of reference can result in different interpretations of the same spatial expression; (b) speakers of different languages may use distinct coordinate frames for non-fronted reference objects; and (c) spatial relations extend beyond exact axes to include acceptable regions.

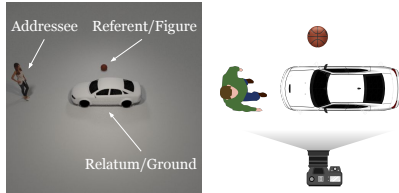| Origin	Frame of Reference	Example (English)
Camera (Preferred)	Egocentric Relative FoR	(From the <u>camera</u>'s viewpoint,) the ball is **behind** the car.
Addressee	Addressee-Centered Relative FoR	(From the <u>woman</u>'s viewpoint,) the ball is to the **left** of the car.
Reference	Object-Centered Intrinsic FoR	(From the <u>car</u>'s viewpoint,) the ball is to the **right** of the car.

Figure 2: An illustrative example of how a frame of reference (FoR) specifies the reference system when describing the spatial relation between a target object (i.e., the ball) and a reference object (i.e., the car). When the FoR is not explicitly specified, English prefers an egocentric relative FoR, i.e., "the ball is behind the car." We study FoRs that lead to ambiguity (Liu et al., 2010).

complicates this ambiguity—different languages employ different conventions in choosing one FoR among multiple competing options. As shown in Figure 1b, speakers may project themselves onto the ball or consider an imaginary listener facing them (Shusterman & Li, 2016). These ambiguities are not easily resolvable based solely on linguistic expressions (Tenbrink, 2004; Liu et al., 2010).

Our main research question is not new: *Do vision-language models represent space, and how?* Several benchmarks (Kamath et al., 2023; Liu et al., 2023a) have been developed for this purpose, consisting of text-image pairs where objects may or may not follow certain spatial relations. However, the aforementioned spatial ambiguities remain largely under-explored when studying VLM-based spatial language understanding and reasoning. We emphasize that FoRs are crucial to studying spatial cognition across modalities, as they provide a foundational framework for understanding how spatial relationships are perceived, interpreted, and communicated (Levinson, 2003).

To fill this gap, we present <u>CO</u>nsistent <u>M</u>ultilingual <u>F</u>rame <u>O</u>f <u>R</u>eference <u>T</u>est (COMFORT), a framework that systematically evaluates the spatial reasoning capabilities of VLMs, emphasizing consistency in understanding ambiguous and disambiguated spatial expressions. COMFORT introduces (1) a set of spatial reasoning tasks instantiated by synthetic 3D images and corresponding text describing spatial relations and (2) metrics to evaluate the robustness and consistency of the model responses. We extend the setup to multilingual settings by evaluating models in 109 languages across 170 regions worldwide. We find that VLMs show alignment with English conventions in spatial language understanding when resolving ambiguities. However, they (1) are still far from achieving robustness and consistency, (2) lack the flexibility to accommodate multiple FoRs, and (3) fail to adhere to linguistic and cultural conventions in cross-lingual tests, as English tends to dominate other languages. With a growing effort to align vision-language models with human cognition, we highlight the ambiguous nature of spatial language and call for increased attention to cross-cultural diversity in spatial reasoning.

2 BACKGROUND AND RELATED WORK

2.1 SPATIAL LANGUAGE AND SPATIAL REPRESENTATION

Some projective terms, such as the English words *front*, *back*, *right*, and *left*, convey meanings of spatial relations (Eschenbach, 2004). These terms articulate the spatial relation between two entities within a designated *frame of reference* (FoR), often involving one entity as the reference object (*relatum/ground*) and another target object (*referent/figure*) that is positioned relative to the relatum

along a specific axis/direction (Levinson, 1996; Frank, 1998). In situated communication, speech act participants (e.g., an *addressee*) may also be considered (Danziger, 2010). To determine acceptable uses of various spatial relations, existing theories suggest that people fit *spatial templates*, which are centered on the relatum and aligned with the FoR (Logan & Sadler, 1996), to parse out *regions of acceptability* of certain directions (Franklin et al., 1995; Carlson-Radvansky & Logan, 1997).

Ambiguities in frame of reference. The choice of perspectives may lead to different FoRs, where Levinson (2003) has identified three main types of FoR: *absolute*, *intrinsic*, and *relative*. The absolute FoR uses cardinal directions, such as *north* and *south*, as fixed bearings. The intrinsic FoR aligns the origin with the relatum, describing the referent's position relative to the relatum's inherent orientation. The relative FoR positions a *viewer* (egocentric or addressee) as the origin, focusing on the observer's intrinsic perspective. Liu et al. (2010) have highlighted the ambiguities in situated communication among three variations of intrinsic and relative FoRs (Figure 2): the *egocentric relative*, the *addressee-centered relative*, and the *object-centered intrinsic* FoRs.[1] When not specified, these FoRs are not easily distinguishable based solely on their linguistic expressions (Tenbrink, 2004). To resolve the ambiguity, individuals from diverse linguistic and cultural backgrounds adopt different preferences and conventions in choosing FoRs (Majid et al., 2004; O'Meara & Báez, 2011; Bohnemeyer et al., 2014; Bender et al., 2020; Ogelo & Bylund, 2024).

Ambiguities in relative FoRs. The variations of relative FoRs form another source of ambiguity. After putting the origin of the coordination system on the viewer, multiple strategies specifying how to transform the axes can be considered (Figure 1b). Different languages use different transformation conventions to resolve the ambiguity of the front-back and left-right of a relatum (Levinson, 2003; Shusterman & Li, 2016), including: (1) *translated* projection (e.g., Hausa) where the coordinate frame of the speaker is directly applied, (2) *rotated* projection (e.g., Tamil), where the coordinate frame of the speaker is transformed with a 180-degree rotation, and (3) *reflected* projection (e.g., English), where only the front-back axis is reversed.

## 2.2 Spatial Understanding in Vision-Language Models

Large language models (LLMs) have exhibited strong adaptability that extends beyond text, encompassing 2D and 3D vision (Tsimpoukelli et al., 2021; Alayrac et al., 2022; Yang et al., 2024), their affordances in the physical embodiment (Driess et al., 2023; Qian et al., 2024), and various other modalities (Yu et al., 2024a). Especially, a variety of vision-language models (VLM) have been developed by visual instruction tuning on paired text-image data (Dai et al., 2023; Liu et al., 2023b; Dong et al., 2024). With supervised fine-tuning using entity-phrase mappings in text-image pairs, grounded VLMs have been developed for fine-grained vision-language understanding at both the region (Chen et al., 2023a; Bai et al., 2023; You et al., 2023; Peng et al., 2024) and pixel level (Lai et al., 2024; Xia et al., 2024; Rasheed et al., 2024; Zhang et al., 2024).

Spatial understanding is known to be challenging even for state-of-the-art VLMs and is receiving increasing attention (Achiam et al., 2023). In addition to using explicit spatial language understanding modules (Rajabi & Kosecka, 2024), recent works such as SpatialVLM (Chen et al., 2024a) and SpatialRGPT (Cheng et al., 2024) improve spatial reasoning in VLMs by leveraging 3D VQA or scene graph data for supervised fine-tuning. Several benchmarks have also been developed to evaluate spatial reasoning in VLMs from various perspectives (Liu et al., 2023a; Cheng et al., 2024; Kamath et al., 2023). Still, these benchmarks overlook ambiguities related to the FoR, lack spatial continuity, and have not proposed metrics to evaluate the robustness and consistency of spatial reasoning.

3 Consistent Multilingual Frame of Reference Test (COMFORT)

We introduce the COnsistent Multilingual Frame Of Reference Test (COMFORT), a new evaluation protocol with dataset, tasks, and comprehensive metrics, to study VLM behaviors in spatial language reasoning with FoR-related ambiguity. This protocol accommodates spatial continuity and various ambiguities, drawing insights from several well-defined metrics to assess performance and prediction consistency. Given our primary focus on analytical and scientific inquiry rather than competitive testing only (Warstadt & Bowman, 2022; Saxon et al., 2024), in this work, we aim to develop better performance and consistency metrics to deepen our understanding of model capabilities.

---

[1]We exclude the absolute FoR from our study as it introduces little ambiguity (Liu et al., 2010).
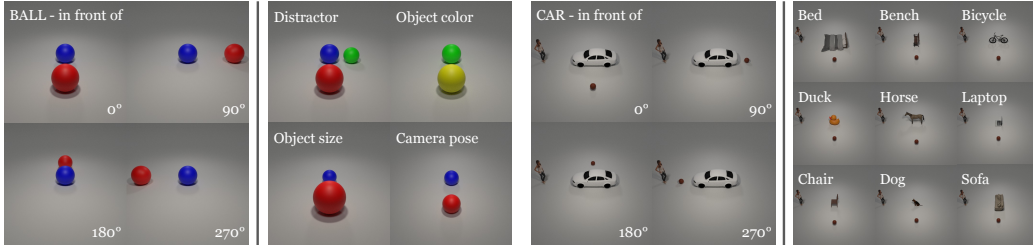
(a) Sample images from COMFORT-BALL. The 4 images on the left are selected every 90° interval along the rotational path out of 36 images. The 4 images on the right illustrate variations with a distractor, different object colors, sizes, or camera poses.

(b) Sample images from COMFORT-CAR. The 4 images on the left are selected every 90° interval along the rotational path out of 36 images. The 9 images on the right are sample images of each variation with different relatum objects.

Figure 3: Examples from the COMFORT-BALL and COMFORT-CAR datasets.

3.1 TASK FORMULATION

Following the setups in object hallucination evaluation (Li et al., 2023; Chen et al., 2024c), we formulate the task as a spatial relation inference problem. In this task, a VLM $\mathcal{M}$ is presented with an RGB image x_{img} and a textual question x_{query}. The image shows the egocentric perception of a scene $s \in \mathcal{S}$, where $\mathcal{S}$ is the set of possible scenes in which the referent moves along a rotational trajectory with a constant radius from the relatum. In contrast to fixing the referents on the standard canonical axes, this setup better mirrors the spatial continuity in common real-world scenarios. A language prompt (Table 1) queries whether a spatial relation $r \in \mathcal{R}$ is satisfied by a referent-relatum pair in the image under FoR $f \in \mathcal{F}$ (Figure 2) in language $\ell \in \mathcal{L}$. This work also examines models using queries with no FoR specified; therefore, a test case in COMFORT is defined as a 4-tuple in $\mathcal{S} \times \mathcal{R} \times (\mathcal{F} \cup \{\emptyset\}) \times \mathcal{L}$. While there are many spatial relations in daily languages, we primarily focus on four canonical directions; that is, the considered relation set $\mathcal{R} = \{\textit{to the left of}, \textit{to the right of}, \textit{in front of}, \textit{behind}\}$. COMFORT covers $|\mathcal{L}| = 109$ languages worldwide; however, we use English as an example to describe the data synthesis and evaluation processes for simplicity and clarity, and refer readers to Appendix A for more details.

3.2 SCENE SETUP

We render the scenes into images using Blender (Blender Online Community, 2016). Each scene consists of a referent and a relatum. The referent follows a rotational trajectory with a constant radius from the relatum to implement spatial continuity. Starting from the canonical front direction, we move the referent with a uniform step of $10°$, totaling up to 36 images per scene. In COMFORT, there are configurations determined by whether the relatum has an intrinsic semantic front:

- **COMFORT-BALL**: When the relatum is non-fronted (e.g., Figure 1b), we focus on the ambiguity of FoR conventions associated with different languages. The split involves an observer's egocentric perception of a referent (e.g., a red ball) and a non-fronted relatum (e.g., a blue ball). We further randomize the dataset with object-level (colors, sizes, and shapes) and scene-level variations (camera positions and distractors) to consider more diverse yet reasonable settings (Figure 3a).

- **COMFORT-CAR**: When the relatum is fronted (e.g., Figure 1a), multiple FoRs can be explicitly adopted to interpret the scene. A COMFORT-CAR image, therefore, involves the egocentric perception of a referent, a fronted relatum, and an additional human addressee. One can interpret the spatial relations using either the Camera, Addressee, or Relatum (C/A/R) as the origin to resolve the reference frame ambiguity. COMFORT-CAR has a set of 10 realistic objects in a typical household or outdoor scene, including *horse*, *car*, *bench*, *laptop*, *rubber duck*, *chair*, *dog*, *sofa*, *bed*, and *bicycle*, all of which have a clear semantic front. We use a basketball as the referent and vary the relatum. In addition to these objects, we include a human addressee in the scene. To disentangle different FoRs as much as possible, we let the addressee face right, and let the relatum face either left or right in the rendered images from the rendering camera's perspective (Figure 3b).

3.3 LANGUAGE QUERY SETUP

Given a pair of referent [A] and a relatum [B], together with a spatial relation of interest, the query is posed as "Is [A] [relation] [B]?" Depending on whether or not and which FoR is specified, the

Origin	Prompt Template
nop	Is [A] [relation] [B]?
cam	From the camera's viewpoint, is [A] [relation] [B]?
add	From the [addressee]'s viewpoint, is [A] [relation] [B]?
rel	From the [relatum]'s viewpoint, is [A] [relation] [B]?

Table 1: The origins of each coordinate system and the corresponding prompt templates for querying the FoR given a referent-relation-relatum triple.
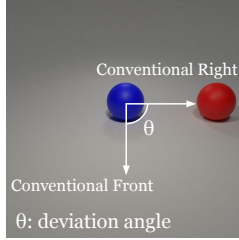

Figure 4: A red ball with a deviation angle $\theta = 90°$ relative to the conventional front (English) of the blue ball.
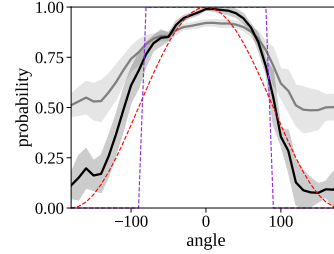

Figure 5: The raw probability $p(\theta)$ in gray, normalized probability $\widehat{p}(\theta)$ in black, and two reference probability $\lambda^{\mathrm{hemi}}(\theta)$ and $\lambda^{\cos}(\theta)$ in red and purple.

query is appended after four different perspective prompts (Table 1): no perspective (nop), camera perspective (cam), addressee perspective (add), and relatum perspective (rel). We only query from the camera egocentric perspective (cam) for COMFORT-BALL, focusing on the ambiguity introduced by variations of the relative FoR. For COMFORT-CAR, we use all four possible language prompts to study how ambiguity in the reference system is resolved. Overall, for English, the above data generation pipeline leads to 720 test cases in COMFORT-BALL, and 57.6k test cases in COMFORT-CAR. The same method for dataset synthesis can be generalized to any other language; however, for computational efficiency, we only include the scenes corresponding to the four most prototypical directions (i.e., left, right, front, and back) in our multilingual analysis.

3.4 PERFORMANCE METRICS

Quantitatively assessing the spatial understanding and reasoning capabilities of models is challenging for two reasons. First, the physical world is continuous, and spatial relations may extend beyond the precise canonical front-back and left-right axes. As noted by Carlson-Radvansky & Logan (1997), there exists *regions of acceptability* where, for instance, an object slightly to the front-left might still be considered being "in front." Second, as Dentella et al. (2023) pointed out, language models are biased towards affirmative responses. However, the intermediate representations may be sensitive to variations in input and, to some extent, align with human perceptions of spatial cues. Based on these concerns and findings, we introduce multiple performance metrics, in addition to the vanilla accuracy, to enable more nuanced analyses.

Unless further clarified, we adopt a right-handed coordinate system with the thumb pointing upwards when describing angles. We define the *deviation angle* $\theta \in (-180°, 180°]$ as the angular displacement from the canonical direction r to the vector connecting the relatum and target. For example, in Figure 4, the deviation angle of canonical right from canonical front is $\theta = 90°$. Following Carlson-Radvansky & Logan (1997), we define the acceptable region for a spatial relation r as the 180-degree hemisphere centered at the corresponding canonical direction. For a VLM $\mathcal{M}$ and a test case indexed by i, we let $P_i(response; \mathcal{M})$ denote the probability of $response \in \{\mathrm{Yes}, \mathrm{No}\}$ assigned by $\mathcal{M}$, and abbreviate it as $P_i(response)$ if there is no confusion.

Accuracy. Given a spatial relation r in the textual prompt, we assess whether the assigned response probabilities correspond to whether the referent lies within the acceptable region defined by the relatum and r. Formally, we define the local probability of the model responding 'Yes' by $p_i = P_i(\mathrm{Yes}) / [P_i(\mathrm{Yes}) + P_i(\mathrm{No})]$. We consider the inference correct if (1) the scene falls into the acceptability region and $p_i > 0.5$ or (2) the scene falls out of the acceptability region and $p_i \leq 0.5$.

Region parsing error. To mitigate the known bias towards affirmative answers, where $\mathbb{E}[p_i] > 0.5$, we normalize it across all image-prompt pairs, resulting in the normalized probability $\widehat{p}_i := (p_i - \min_j p_j)/(\max_j p_j - \min_j p_j)$. We adopt the root mean square error (RMSE) between the normalized acceptance probability $\widehat{p}$ and reference probability threshold λ^{ref} that represents the actual regions of acceptability, $\varepsilon^{\mathrm{ref}} = \sqrt{\sum_{i=1}^{n} (\widehat{p}_i - \lambda^{\mathrm{ref}})^2 / n}$, where λ^{ref} denotes the reference of the assigned probability, analogically to ground-truth labels in machine learning terms.

We introduce two analytically and geometrically motivated proposals defining λ^{ref}, λ^{hemi} and $\lambda^{\cos}$, based on hemispheres and cosine of angles, respectively. First, the hemisphere-based reference λ^{hemi} is defined as $\lambda^{\mathrm{hemi}}(\theta) := \mathbb{1}[\theta \in (-90°, 90°)]$. Here, $\theta = 0°$ corresponds to the most prototypical
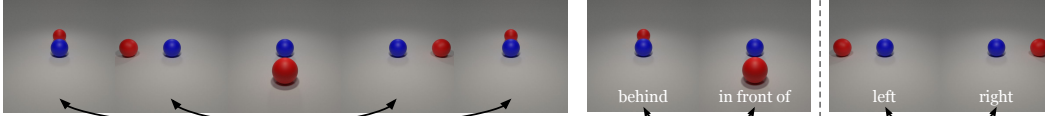
(a) An illustration of the spatial symmetry with respect to the (conventional) front. As the red ball rotates around the blue ball, spatial symmetry consistency ensures that each symmetric pair, with different deviation angles θ and $-\theta$, has the same probability of being identified as the front.

(b) Antonyms for spatial opposite consistency, e.g., When evaluating if the red ball is to the left of the blue ball, spatial opposite consistency ensures the probability of accepting a sample as left equals the probability of identifying it as not right.

Figure 6: Illustrations for the consistency metrics defined in COMFORT.

spatial relation, and $\theta = 180°$ corresponds to the opposite. Intuitively, $\lambda^{\text{hemi}} = 1$ denotes the test case falls into the acceptable region defined by the textual prompt, and otherwise not. The second reference is derived from the cosine of the deviation angle. Matching the range of the cosine function to that of probability, i.e., $[0, 1]$, we define the cosine-based reference $\lambda^{\cos}(\theta)$ by $\lambda^{\cos}(\theta) := [\cos(\theta) + 1]/2$.

Figure 5 shows an example of the vanilla probability curve $p(\theta)$ from LLaVA-v1.5-7B (Liu et al., 2023b), normalized probability curve $\widehat{p}(\theta)$, and two reference curves $\lambda^{\text{hemi}}(\theta)$ and $\lambda^{\cos}(\theta)$. We report both $\varepsilon^{\text{hemi}}(\theta)$ and $\varepsilon^{\cos}(\theta)$ in experiments. We also note that in human spatial cognition, the regions of acceptability are neither mutually exclusive 90° quadrants nor overlapping 180° hemispheres, as they vary across individuals and depend on the situational context (Franklin et al., 1995).

3.5 ROBUSTNESS METRICS

Standard deviation. In COMFORT, some images depict variations of the same scene, sharing identical spatial relations between the referent and the object but differing in terms of object colors, sizes, or distractors. When the spatial relation and the query text remain unchanged, an ideal model should have consistent predictions for all variations. To measure model robustness, we report the average standard deviation of the predicted probability $\widehat{p}_i$ across all deviation angles $\sigma := \text{avg}_\theta \sigma(\theta)$.

Prediction noise. Since our data is generated through interpolation, ideally, if a model well understands spatial relations, the probability curve with respect to the deviation angle should be low-frequency (i.e., smooth) rather than high-frequency (i.e., noisy). Therefore, we measure the noise by the RMSE, denoted by η, between the predicted probability and a Butterworth Low Pass Filter (LPF; Butterworth et al., 1930): $\eta := \sqrt{\sum_{i=1}^{n} [\widehat{p}_i - \text{LPF}(\widehat{p}_i)]^2/n}$. A smaller value of η indicates that the probabilities are changing more smoothly, which is more desirable.

3.6 CONSISTENCY METRICS

Spatial symmetric consistency. A critical aspect of consistent spatial reasoning is geometric symmetry. As our tested target object rotates around the relatum in a circular path that is spatially symmetric, we expect the probabilities of an ideal VLM to consistently reflect geometric symmetry (Figure 6a). For a pair of test cases, indexed by i and j, that have the same configurations but opposite deviation angles, i.e., $\theta_i + \theta_j = 0°$, we define the symmetry consistency: $c^{\text{sym}} := \sqrt{2 \sum_{i,j} (\widehat{p}_i - \widehat{p}_j)^2/(n-1)}$.

Spatial opposite consistency. Similarly, we expect the probabilities of an ideal VLM to consistently reflect geometric opposition (Figure 6b). For example, the probability that a sample is accepted by the spatial relation "to the left" should be identical to the probability that it is rejected by "to the right." For a pair of opposite spatial relation $r, \text{opp}(r) \in \mathcal{R}$ with the same configurations including the deviation angles θ_i, the opposition consistency is given as: $c^{\text{opp}} := \sqrt{\sum_{i=0}^{n} (\widehat{p}_i^r + \widehat{p}_i^{\text{opp}(r)} - 1)^2/n}$.

4 EMPIRICAL EXPERIMENTS AND MAIN FINDINGS

The COMFORT framework enables us to investigate whether the internal representations of vision-language models encode spatial relations, and if they do, which underlying coordinate systems these representations capture. This can further be broken down into two research questions: (1) When presented with an ambiguous spatial expression, do VLMs follow conventions and exhibit specific preferred FoRs (and the coordinate transformation in relative FoRs) to resolve the ambiguity? (2) How effectively can VLMs adopt different FoRs, when perspectives are explicitly specified to disambiguate spatial expressions paired with visual scenes?

Model	Back ε^{cos} ($\downarrow$)		Front ε^{cos} ($\downarrow$)		Left ε^{cos} ($\downarrow$)		Right ε^{cos} ($\downarrow$)		Aggregated			Preferred
	Same	**Rev.**	Same	**Rev.**	**Same**	Rev.	**Same**	Rev.	Tran.	Rot.	**Ref.**	
InstructBLIP-7B	45.6	**39.0**	31.6	52.0	**37.2**	48.0	47.5	**37.8**	**40.5**	44.2	43.9	-
InstructBLIP-13B	**40.9**	45.5	46.0	**37.4**	**43.4**	44.9	45.6	**41.6**	44.0	**42.3**	43.0	-
mBLIP-BLOOMZ	**51.2**	53.7	51.2	**47.9**	**52.4**	53.5	54.6	**46.8**	52.3	**50.5**	52.1	-
GLaMM	58.3	**33.3**	43.9	**42.9**	**38.3**	51.8	**17.3**	63.7	39.5	47.9	**33.0**	**Ref.**
LLaVA-1.5-7B	54.0	**32.9**	59.1	**24.8**	**11.9**	70.0	**13.0**	68.5	34.5	49.0	**20.7**	**Ref.**
LLaVA-1.5-13B	61.8	**19.2**	56.0	**27.7**	**31.7**	61.8	**24.3**	64.3	43.4	43.2	**25.7**	**Ref.**
XComposer2	73.2	**17.9**	74.5	**20.7**	**20.1**	80.9	**21.3**	81.1	47.3	50.1	**20.0**	**Ref.**
MiniCPM-V	70.9	**21.9**	64.3	**26.9**	**19.7**	74.1	**21.1**	73.3	44.0	49.1	**22.4**	**Ref.**
GPT-4o	75.7	**28.2**	73.6	**32.0**	**24.3**	80.8	**25.1**	80.8	49.7	55.5	**27.4**	**Ref.**

Table 2: Preferred coordinate transformation mapping from the egocentric viewer (camera) to the relatum in the relative FoR. The cosine region parsing errors ε^{cos} are computed against both the Same and Reversed directions relative to the egocentric viewer's coordinate system. For example, native English speakers typically prefer a Reflected transformation, which maintains the lateral (left/right) axis but reverses the sagittal (front/back) axis relative to the viewer (Figure 1). We determine the preferred transformation based on the aggregated performance, with "-" for no significant preference.

Model	Back ε^{cos} ($\downarrow$)			Front ε^{cos} ($\downarrow$)			Left ε^{cos} ($\downarrow$)			Right ε^{cos} ($\downarrow$)			Aggregated			Prefer
	Ego.	Int.	Add.	**Ego.**	Int.	Add.	**Ego.**	Int.	Add.	**Ego.**	Int.	Add.	**Ego.**	Int.	Add.	
InstructBLIP-7B	41.0	**38.6**	**38.6**	**40.9**	46.9	46.9	45.6	**32.5**	51.9	39.6	51.2	**31.8**	**41.8**	42.3	42.3	-
InstructBLIP-13B	**32.9**	34.4	34.4	52.5	**48.5**	**48.5**	47.8	56.2	**27.8**	40.6	**27.6**	56.6	43.5	**41.7**	41.8	-
mBLIP-BLOOMZ	**52.2**	53.2	53.2	45.3	**44.6**	**44.6**	47.8	**47.6**	48.1	45.4	48.4	**42.4**	47.7	48.4	**47.1**	-
GLaMM	**28.0**	49.1	49.1	**30.0**	40.2	40.2	**14.0**	56.8	41.5	**13.7**	53.0	46.6	**21.4**	49.8	44.4	**Ego.**
LLaVA-1.5-7B	**20.9**	43.0	43.0	34.5	**32.6**	**32.6**	**13.4**	53.5	47.4	**14.3**	53.6	49.3	**20.8**	45.7	43.1	**Ego.**
LLaVA-1.5-13B	**31.9**	38.8	38.8	**24.8**	57.1	57.1	**11.7**	51.1	51.1	27.5	57.4	48.7	**24.0**	51.1	48.9	**Ego.**
XComposer2	**12.7**	49.3	49.3	**15.2**	48.3	48.3	**18.8**	61.2	53.7	**16.5**	58.4	54.5	**15.8**	54.3	51.4	**Ego.**
MiniCPM-V	**34.2**	40.7	40.7	**35.5**	53.4	53.4	**18.0**	53.9	58.4	**19.0**	58.1	52.7	**26.7**	51.5	51.3	**Ego.**
GPT-4o	38.3	**36.7**	**36.7**	**43.1**	50.2	50.2	**34.7**	59.3	56.5	**24.3**	57.3	61.7	**35.1**	50.9	51.3	**Ego.**

Table 3: Preferred frame of reference in VLMs. Models' Cosine Region Parsing Errors ε^{cos} are computed against the Intrinsic FoR (relatum origin), Egocentric relative FoR (camera origin), and Addressee-centric relative FoR (addressee origin). English typically prefers an egocentric relative FoR. We determine the preferred FoR based on the aggregated performance, with "-" indicating no significant preference.

In principle, COMFORT can be applied to all VLMs, whether multilingual or monolingual. We note that most existing open-source VLMs are English-based language models; therefore, we begin our experiments on English conventions, where both *relative* and *intrinsic* FoRs are available, but there is a conventional preference for a *relative* FoR combined with a *reflected* coordinate transformation in the relative FoR (see Levinson, 2003, Table 5.4). We further extend our setup to multilingual settings by evaluating models in 109 languages across 170 regions worldwide. To cover a variety of VLMs with different capabilities and training approaches, we evaluate the following models:

- VLMs build from supervised instruction fine-tuning: InstructBLIP-7B/13B- (Dai et al., 2023), LLaVA-v1.5-7B/13B (Liu et al., 2023b), InternLM-XComposer2-7B (Dong et al., 2024);
- VLMs with both supervised fine-tuning and reinforcement learning alignment: MiniCPM-Llama3-V-v2.5-8B (Hu et al., 2024; Yu et al., 2024b);
- Mechanistically grounded VLMs: GLaMM-7B (Rasheed et al., 2024);
- Multilingual VLMs[2]: mBLIP-BLOOMZ-7B (Geigle et al., 2024) and GPT-4o (OpenAI, 2024).

4.1 MOST VLMs PREFER REFLECTED COORDINATE TRANSFORMATION CONVENTION

In this section, we address the research question: **do VLMs have a preferred coordinate transformation convention, and if so, what is it?** Experiments are conducted on COMFORT-BALL using the camera perspective prompt (cam) that explicitly specifies an egocentric relative FoR (Table 2). Table 7 in the appendix shows the complete evaluation including ε^{hemi} and ε^{cos}.

We observe that almost all VLMs demonstrate a clear preference over the *reflected* transformation similar to English, except the BLIP series. Still, some models are also affected by the ambiguity of multiple transformation conventions. With the textual prompting specifying a relation, at $\theta = 0$, GPT-4o and LLaVA-1.5-13B show a sharp drop of performance and a significant variance for behind and right, respectively (Figure 7), indicating that some models are sensitive to other transformations.

[2]The PaLI series (Chen et al., 2023c;b; 2024b) are closed sourced.

Language		English	Tamil	Hausa
Intrinsic		50.9	52.0	54.0
Ego-Rel	Ref.	**35.8**	**40.4**	**41.0**
	Rot.	57.3	55.2	56.1
	Tran.	53.7	51.1	53.0
Add-Rel	Ref.	58.8	52.2	52.8
	Rot.	51.3	52.9	55.3
	Tran.	56.1	56.1	56.1
GPT-4o Prefer		Ego-Ref.	Ego-Ref.	Ego-Ref.
Human Prefer		Ego-Ref.	Ego-Rot.	Ego-Trans.
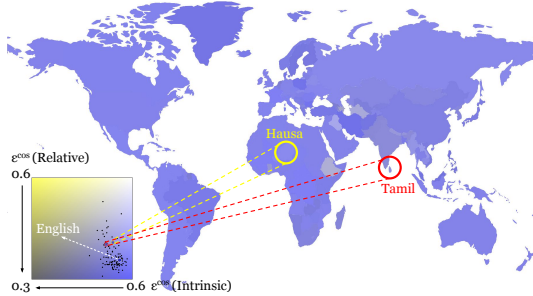
Figure 8: GPT-4o's preferences for intrinsic FoR over the relative FoR across regions. The plot is based on the top three spoken languages in each region, as reported by The World Factbook (Central Intelligence Agency, 2009), and averages the cosine parsing error (ε^{cos}, ↓), weighted by the speaking population. We present a quantitative comparison of English, Tamil, and Hausa, with the best-performing FoR marked in bold and the convention preferred by human speakers underlined.

in the appendix gives the complete evaluation. We find that all models, including the strong ones like GPT-4 and InternLM-XComposer2, show close-to-chance performance (50% accuracy) when being prompted to use the intrinsic or addressee-centered relative FoRs. Compared to the same probing setup without a perspective specified (nop), we find generally marginal improvements in region parsing error (ε), whereas the accuracy decreases. Overall, the results indicate that while VLMs can comprehend scenes using egocentric relative FoR, they struggle to adapt flexibly to alternative FoRs.

4.4 SPATIAL REPRESENTATIONS IN VLMS ARE NOT ROBUST AND CONSISTENT

In this section, we further ask: **are spatial representations in VLMs robust and consistent?** The considered metrics include accuracy (Acc), region parsing error (ε), prediction noise (η), standard deviation (σ), and consistency (c) as defined in Section 3. One commonly considered possibility that VLMs underperform is that they suffer from *object hallucination*, where they misperceive objects in the scenes (Li et al., 2023; Chen et al., 2024c). Following the object probing setups, we prompt the VLMs to inquire about the presence of an existing object and a non-existing object in the scene, and compute the F1-score (Table 5). We find that the BLIP models suffer from severe object hallucinations, which contribute to their underperformance in the previous evaluation. Many VLMs, despite showing decent performance metrics in terms of spatial understanding and reasoning accuracy, demonstrate a lack of robustness and consistency. For example, the spatial opposite consistency (c^{opp}) of GPT-4 is not significantly better than 30 random trials. In contrast, VLMs that have undergone supervised fine-tuning on spatial relation tasks have a more robust and consistent spatial representation. For instance, InternLM-XComposer2 and MiniCPM-V (on the COMFORT-BALL task, with no object hallucinations) show improved performance. On the other hand, although GLaMM is mechanistically grounded to objects and exhibits minimal object hallucination, its spatial understanding capability is poor. This suggests that improving visual entity grounding helps in recognizing individual objects but does not automatically translate to better spatial understanding between multiple objects.

4.5 A CROSS-LINGUAL AND CROSS-CULTURAL EVALUATION OF FRAME OF REFERENCE

All previous experiments are centered around English; however, individuals from diverse multilingual and cultural backgrounds may adopt different preferences and conventions to select their FoR in resolving ambiguities (Majid et al., 2004; O'Meara & Báez, 2011; Bohnemeyer et al., 2014; Ogelo & Bylund, 2024). Our next research question naturally arises: **Do multilingual VLMs faithfully follow the preferences and conventions (associated with different languages) to select the FoR?** To extend the study of preferred FoR from English to a multilingual setting, we evaluate 109 languages worldwide to investigate whether each language shows a preferred FoR. We translate the English prompts into the target languages using the Google Cloud Translate API. Given that the open-source language models either lack strong multilingual capabilities or underperform in previous evaluations, we study this problem on the GPT-4o model (OpenAI, 2024). We follow the setup similar to Section 4.2, but only evaluate the images corresponding to the four canonical directions using the nop prompt. For each language, we compute ε^{cos} for each FoR and coordinate transformation. Figure 8 presents a visualization of the world map, displaying the preference of each region for using the (object-centered) intrinsic FoR over the relative FoR, where the latter corresponds to a low ε^{cos} value. Table 10 in the Appendix summarizes the results across all tested languages.

Nearly all tested languages demonstrate a preference towards the relative FoR, except several underrepresented languages, such as Konkani, Kurdish, and Amharic, which exhibit near-random performance without a significant preference. In Figure 8, we present a classic comparison between English, Tamil, and Hausa similar to that of Levinson (2003), with the best-performing FoR marked in bold, and the preferred convention by humans underlined. Although human speakers of these languages have different preferred coordinate transformation conventions, the English convention of reflected projection is observed for both Tamil and Hausa. Although, for example, Hausa permits an English-like interpretation of front-back relations, this interpretation is generally less favored and may confuse Hausa speakers (Hill, 1982). This raises concerns that English may dominate the FoR preference conventions of other languages in multilingual VLMs.

5 DISCUSSIONS

Do vision-language models represent space and how? It is insufficient to answer this question by simply querying the model with text-image pairs and comparing the output with a fixed ground truth. We must, at least, query the models with awareness of the ambiguity in FoRs, which is essential in determining how the scenes in the physical world are mapped to spatial expressions (Levinson, 2003). Our experiments confirm that many VLMs are equipped with reasonable spatial representations through vision-language training alone; in particular, most VLMs clearly prefer the egocentric relative FoR with reflected projection, aligning with English conventions. However, our results also show these representations lack robustness and consistency in a continuous space. Similar experimental setups can yield widely varying performance across different spatial relations—for example, GPT-4 shows minimal preferences for the egocentric relative FoR along the sagittal axis but a significant preference along the lateral one (Table 3). As a result, VLMs demonstrate unsatisfactory consistency in their spatial performance (Table 5). Future work is necessary to improve the consistency and robustness of spatial representations in these models.

Perspective taking as a prerequisite of human-like spatial reasoning. Most languages support multiple FoRs.[3] The ability to understand and reason about space from a non-egocentric perspective is an important foundation of the Theory of Mind, a basic building block of our situated communication skill that allows us to infer others' mental states (Ma et al., 2023b). One of our key findings is that VLMs still struggle to adopt alternative FoRs flexibly, even when provided with explicit perspective-taking instructions (Section 4.3). We hypothesize that this phenomenon may come from a reporting bias in the image-text datasets available on the internet—it is natural to take the reflected relative FoR to view images presented on a screen, but this does not always apply in real-world applications. To address this issue, we suggest future work extend the current 2D VLMs to the 3D domain, by considering camera poses and multiview data (Yang et al., 2024; Hao et al., 2024) for training.

Cross-cultural conventions in cross-lingual spatial understanding. The conventions for resolving spatial ambiguities are not uniform, as individuals from diverse linguistic and cultural backgrounds select their FoR differently. Cultural conventions can even be transmitted as individuals are exposed to other languages. Bohnemeyer et al. (2014) found that among indigenous language speakers with various preferences in FoRs, those more proficient in Spanish tend to use the reflected relative FoR (Spanish convention) more in their native language. This phenomenon has led to their Linguistic Transmission Hypothesis: "Using any language or linguistic variety – independently of its structures – may facilitate the acquisition of cultural practices of nonlinguistic cognition shared among the speakers of the language." Analogously, our experiment raises important concerns that English may dominate the FoR preference conventions of other languages in multilingual VLMs. This is not surprising, as current training recipes for multilingual multimodal language models heavily rely on machine-translated captions (Chen et al., 2023c; Geigle et al., 2024); however, this practice can be problematic: for instance, Hausa prefers an interpretation where the "front" aligns with the English concept of "back," (Hill, 1982), where this approach may lead to English conventions overshadowing those of other languages. At a high level, this issue is not limited to spatial reasoning: as an example, Shi et al. (2023) have demonstrated that English is always the best chain-of-thought language for math reasoning with multilingual LLMs, no matter what language is used for the problem description. To enable similar linguistic transmission in AI models, exposure to naturally generated multilingual image-text data is crucial (Romero et al., 2024).

---

[3]Some languages, in very rare cases, have only one available spatial frame of reference. For example, Guugu Yimithirr exclusively uses the absolute FoR (Levinson, 2003).

ACKNOWLEDGMENTS

REFERENCES

Josh Achiam, Steven Adler, Sandhini Agarwal, Lama Ahmad, Ilge Akkaya, Florencia Leoni Aleman, Diogo Almeida, Janko Altenschmidt, Sam Altman, Shyamal Anadkat, et al. Gpt-4 technical report. *arXiv preprint arXiv:2303.08774*, 2023.

Jean-Baptiste Alayrac, Jeff Donahue, Pauline Luc, Antoine Miech, Iain Barr, Yana Hasson, Karel Lenc, Arthur Mensch, Katherine Millican, Malcolm Reynolds, et al. Flamingo: a visual language model for few-shot learning. *Advances in neural information processing systems*, 35:23716–23736, 2022.

Jinze Bai, Shuai Bai, Shusheng Yang, Shijie Wang, Sinan Tan, Peng Wang, Junyang Lin, Chang Zhou, and Jingren Zhou. Qwen-vl: A frontier large vision-language model with versatile abilities. *arXiv preprint arXiv:2308.12966*, 2023.

Andrea Bender, Sarah Teige-Mocigemba, Annelie Rothe-Wulf, Miriam Seel, and Sieghard Beller. Being *In Front* is good—but where is *In Front*? preferences for spatial referencing affect evaluation. *Cognitive Science*, 44(6):e12840, 2020.

Blender Online Community. Blender - a 3d modelling and rendering package. *Blender Foundation, Blender Institute*, 2016.

Jürgen Bohnemeyer, Katharine Donelson, Randi Tucker, Elena Benedicto, Alejandra Capistrán Garza, Alyson Eggleston, Néstor Hernández Green, María de Jesús Selene Hernández Gómez, Samuel Herrera Castro, Carolyn O'Meara, et al. The cultural transmission of spatial cognition: Evidence from a large-scale study. In *Proceedings of the Annual Meeting of the Cognitive Science Society*, volume 36, 2014.

Stephen Butterworth et al. On the theory of filter amplifiers. *Wireless Engineer*, 7(6):536–541, 1930.

Laura A Carlson-Radvansky and Gordon D Logan. The influence of reference frame selection on spatial template construction. *Journal of memory and language*, 37(3):411–437, 1997.

Central Intelligence Agency. *The world factbook 2009*. Central Intelligence Agency, 2009. `https://www.cia.gov/the-world-factbook/field/languages/` [Accessed: (Jun 1st 2024)].

Boyuan Chen, Zhuo Xu, Sean Kirmani, Brain Ichter, Dorsa Sadigh, Leonidas Guibas, and Fei Xia. Spatialvlm: Endowing vision-language models with spatial reasoning capabilities. In *Proceedings of the IEEE/CVF Conference on Computer Vision and Pattern Recognition*, pp. 14455–14465, 2024a.

Keqin Chen, Zhao Zhang, Weili Zeng, Richong Zhang, Feng Zhu, and Rui Zhao. Shikra: Unleashing multimodal llm's referential dialogue magic. *arXiv preprint arXiv:2306.15195*, 2023a.

Xi Chen, Xiao Wang, Lucas Beyer, Alexander Kolesnikov, Jialin Wu, Paul Voigtlaender, Basil Mustafa, Sebastian Goodman, Ibrahim Alabdulmohsin, Piotr Padlewski, et al. Pali-3 vision language models: Smaller, faster, stronger. *arXiv preprint arXiv:2310.09199*, 2023b.

Xi Chen, Xiao Wang, Soravit Changpinyo, AJ Piergiovanni, Piotr Padlewski, Daniel Salz, Sebastian Goodman, Adam Grycner, Basil Mustafa, Lucas Beyer, Alexander Kolesnikov, Joan Puigcerver, Nan Ding, Keran Rong, Hassan Akbari, Gaurav Mishra, Linting Xue, Ashish V Thapliyal, James Bradbury, Weicheng Kuo, Mojtaba Seyedhosseini, Chao Jia, Burcu Karagol Ayan, Carlos Riquelme Ruiz, Andreas Peter Steiner, Anelia Angelova, Xiaohua Zhai, Neil Houlsby, and Radu Soricut. Pali: A jointly-scaled multilingual language-image model. In *The Eleventh International Conference on Learning Representations*, 2023c.

Xi Chen, Josip Djolonga, Piotr Padlewski, Basil Mustafa, Soravit Changpinyo, Jialin Wu, Carlos Riquelme Ruiz, Sebastian Goodman, Xiao Wang, Yi Tay, et al. On scaling up a multilingual vision and language model. In *Proceedings of the IEEE/CVF Conference on Computer Vision and Pattern Recognition*, pp. 14432–14444, 2024b.

Xuweiyi Chen, Ziqiao Ma, Xuejun Zhang, Sihan Xu, Shengyi Qian, Jianing Yang, David F Fouhey, and Joyce Chai. Multi-object hallucination in vision-language models. In *The Thirty-eighth Annual Conference on Neural Information Processing Systems*, 2024c.

An-Chieh Cheng, Hongxu Yin, Yang Fu, Qiushan Guo, Ruihan Yang, Jan Kautz, Xiaolong Wang, and Sifei Liu. Spatialrgpt: Grounded spatial reasoning in vision-language models. *arXiv preprint arXiv:2406.01584*, 2024.

Wenliang Dai, Junnan Li, Dongxu Li, Anthony Meng Huat Tiong, Junqi Zhao, Weisheng Wang, Boyang Li, Pascale N Fung, and Steven Hoi. Instructblip: Towards general-purpose vision-language models with instruction tuning. In *Advances in Neural Information Processing Systems*, volume 36, 2023.

Eve Danziger. Deixis, gesture, and cognition in spatial frame of reference typology. *Studies in Language. International Journal sponsored by the Foundation "Foundations of Language"*, 34(1): 167–185, 2010.

Vittoria Dentella, Fritz Günther, and Evelina Leivada. Systematic testing of three language models reveals low language accuracy, absence of response stability, and a yes-response bias. *Proceedings of the National Academy of Sciences*, 120(51):e2309583120, 2023.

Xiaoyi Dong, Pan Zhang, Yuhang Zang, Yuhang Cao, Bin Wang, Linke Ouyang, Xilin Wei, Songyang Zhang, Haodong Duan, Maosong Cao, et al. Internlm-xcomposer2: Mastering free-form text-image composition and comprehension in vision-language large model. *arXiv preprint arXiv:2401.16420*, 2024.

Danny Driess, Fei Xia, Mehdi SM Sajjadi, Corey Lynch, Aakanksha Chowdhery, Brian Ichter, Ayzaan Wahid, Jonathan Tompson, Quan Vuong, Tianhe Yu, et al. Palm-e: An embodied multimodal language model. In *International Conference on Machine Learning*, pp. 8469–8488. PMLR, 2023.

Carola Eschenbach. Contextual, functional, and geometric components in the semantics of projective terms. In *Functional Features in Language and Space: Insights from Perception, Categorization, and Development*. Oxford University Press, 12 2004.

Andrew U Frank. Formal models for cognition—taxonomy of spatial location description and frames of reference. *Spatial cognition: An interdisciplinary approach to representing and processing spatial knowledge*, pp. 293–312, 1998.

Nancy Franklin, Linda A Henkel, and Thomas Zangas. Parsing surrounding space into regions. *Memory & Cognition*, 23:397–407, 1995.

Gregor Geigle, Abhay Jain, Radu Timofte, and Goran Glavaš. mblip: Efficient bootstrapping of multilingual vision-llms. In *Proceedings of the 3rd Workshop on Advances in Language and Vision Research (ALVR)*, pp. 7–25, 2024.

Dedre Gentner, Asli Özyürek, Özge Gürcanli, and Susan Goldin-Meadow. Spatial language facilitates spatial cognition: Evidence from children who lack language input. *Cognition*, 127(3):318–330, 2013.

Tianrui Guan, Fuxiao Liu, Xiyang Wu, Ruiqi Xian, Zongxia Li, Xiaoyu Liu, Xijun Wang, Lichang Chen, Furong Huang, Yaser Yacoob, et al. Hallusionbench: an advanced diagnostic suite for entangled language hallucination and visual illusion in large vision-language models. In *Proceedings of the IEEE/CVF Conference on Computer Vision and Pattern Recognition*, pp. 14375–14385, 2024.

Shengyu Hao, Wenhao Chai, Zhonghan Zhao, Meiqi Sun, Wendi Hu, Jieyang Zhou, Yixian Zhao, Qi Li, Yizhou Wang, Xi Li, et al. Ego3dt: Tracking every 3d object in ego-centric videos. In *Proceedings of the 32nd ACM International Conference on Multimedia*, pp. 2945–2954, 2024.

William G Hayward and Michael J Tarr. Spatial language and spatial representation. *Cognition*, 55 (1):39–84, 1995.

Clifford Hill. Up/down, front/back, left/right. a contrastive study of hausa and english. *Here and there: Cross-linguistic studies on deixis and demonstration*, 1342, 1982.

Shengding Hu, Yuge Tu, Xu Han, Chaoqun He, Ganqu Cui, Xiang Long, Zhi Zheng, Yewei Fang, Yuxiang Huang, Weilin Zhao, et al. Minicpm: Unveiling the potential of small language models with scalable training strategies. *arXiv preprint arXiv:2404.06395*, 2024.

Chuanyang Jin, Yutong Wu, Jing Cao, Jiannan Xiang, Yen-Ling Kuo, Zhiting Hu, Tomer Ullman, Antonio Torralba, Joshua Tenenbaum, and Tianmin Shu. MMTom-QA: Multimodal theory of mind question answering. In *Proceedings of the 62nd Annual Meeting of the Association for Computational Linguistics (Volume 1: Long Papers)*, pp. 16077–16102, 2024.

Amita Kamath, Jack Hessel, and Kai-Wei Chang. What's "up" with vision-language models? investigating their struggle with spatial reasoning. In *EMNLP*, 2023.

Adam Kendon. Spacing and orientation in co-present interaction. *Development of Multimodal Interfaces: Active Listening and Synchrony: Second COST 2102 International Training School, Dublin, Ireland, March 23-27, 2009, Revised Selected Papers*, pp. 1–15, 2010.

Xin Lai, Zhuotao Tian, Yukang Chen, Yanwei Li, Yuhui Yuan, Shu Liu, and Jiaya Jia. Lisa: Reasoning segmentation via large language model. In *Proceedings of the IEEE/CVF Conference on Computer Vision and Pattern Recognition*, pp. 9579–9589, 2024.

Stephen C Levinson. Frames of reference and molyneux's question: Crosslinguistic evidence. *Language and Space*, pp. 109–170, 1996.

Stephen C Levinson. *Space in language and cognition: Explorations in cognitive diversity*, volume 5. Cambridge University Press, 2003.

Yifan Li, Yifan Du, Kun Zhou, Jinpeng Wang, Wayne Xin Zhao, and Ji-Rong Wen. Evaluating object hallucination in large vision-language models. In *Proceedings of the 2023 Conference on Empirical Methods in Natural Language Processing*, 2023.

Changsong Liu, Jacob Walker, and Joyce Y Chai. Ambiguities in spatial language understanding in situated human robot dialogue. In *2010 AAAI Fall Symposium Series*, 2010.

Fangyu Liu, Guy Emerson, and Nigel Collier. Visual spatial reasoning. *Transactions of the Association for Computational Linguistics*, 11:635–651, 2023a.

Haotian Liu, Chunyuan Li, Qingyang Wu, and Yong Jae Lee. Visual instruction tuning. In *Advances in neural information processing systems*, volume 36, 2023b.

Yuan Liu, Haodong Duan, Yuanhan Zhang, Bo Li, Songyang Zhang, Wangbo Zhao, Yike Yuan, Jiaqi Wang, Conghui He, Ziwei Liu, et al. Mmbench: Is your multi-modal model an all-around player? *arXiv preprint arXiv:2307.06281*, 2023c.

Gordon D Logan and Daniel D Sadler. A computational analysis of the apprehension of spatial relations. *Language and Space*, pp. 493–530, 1996.

Ziqiao Ma, Jiayi Pan, and Joyce Chai. World-to-words: Grounded open vocabulary acquisition through fast mapping in vision-language models. In *Proceedings of the 61st Annual Meeting of the Association for Computational Linguistics (Volume 1: Long Papers)*, pp. 524–544, 2023a.

Ziqiao Ma, Jacob Sansom, Run Peng, and Joyce Chai. Towards a holistic landscape of situated theory of mind in large language models. *Findings of Empirical Methods in Natural Language Processing*, 2023b.

Zixian Ma, Jerry Hong, Mustafa Omer Gul, Mona Gandhi, Irena Gao, and Ranjay Krishna. Crepe: Can vision-language foundation models reason compositionally? In *Proceedings of the IEEE/CVF Conference on Computer Vision and Pattern Recognition*, pp. 10910–10921, 2023c.

Asifa Majid, Melissa Bowerman, Sotaro Kita, Daniel BM Haun, and Stephen C Levinson. Can language restructure cognition? the case for space. *Trends in cognitive sciences*, 8(3):108–114, 2004.

Roshanak Mirzaee and Parisa Kordjamshidi. Transfer learning with synthetic corpora for spatial role labeling and reasoning. In *Proceedings of the 2022 Conference on Empirical Methods in Natural Language Processing*, pp. 6148–6165, Abu Dhabi, United Arab Emirates, December 2022. Association for Computational Linguistics. URL https://aclanthology.org/2022.emnlp-main.413.

Roshanak Mirzaee, Hossein Rajaby Faghihi, Qiang Ning, and Parisa Kordjamshidi. SPARTQA: A textual question answering benchmark for spatial reasoning. In *Proceedings of the 2021 Conference of the North American Chapter of the Association for Computational Linguistics: Human Language Technologies*, pp. 4582–4598, Online, June 2021. Association for Computational Linguistics. doi: 10.18653/v1/2021.naacl-main.364. URL https://aclanthology.org/2021.naacl-main.364.

Reinhard Moratz and Thora Tenbrink. Spatial reference in linguistic human-robot interaction: Iterative, empirically supported development of a model of projective relations. *Spatial cognition and computation*, 6(1):63–107, 2006.

Edward Munnich, Barbara Landau, and Barbara Anne Dosher. Spatial language and spatial representation: A cross-linguistic comparison. *Cognition*, 81(3):171–208, 2001.

Awino Ogelo and Emanuel Bylund. Spatial frames of reference in dholuo. *Language Sciences*, 104: 101614, 2024.

OpenAI. Hello gpt-4o, May 2024. URL https://openai.com/index/hello-gpt-4o/.

Carolyn O'Meara and Gabriela Pérez Báez. Spatial frames of reference in mesoamerican languages. *Language Sciences*, 33(6):837–852, 2011.

Zhiliang Peng, Wenhui Wang, Li Dong, Yaru Hao, Shaohan Huang, Shuming Ma, Qixiang Ye, and Furu Wei. Grounding multimodal large language models to the world. In *The Twelfth International Conference on Learning Representations*, 2024.

Tanawan Premsri and Parisa Kordjamshidi. Neuro-symbolic training for reasoning over spatial language. In *Proceedings of NAACL-2025*. Association for Computational Linguistics, 2025.

Shannon M Pruden, Susan C Levine, and Janellen Huttenlocher. Children's spatial thinking: Does talk about the spatial world matter? *Developmental science*, 14(6):1417–1430, 2011.

Jennie E Pyers, Anna Shusterman, Ann Senghas, Elizabeth S Spelke, and Karen Emmorey. Evidence from an emerging sign language reveals that language supports spatial cognition. *Proceedings of the National Academy of Sciences*, 107(27):12116–12120, 2010.

Shengyi Qian, Weifeng Chen, Min Bai, Xiong Zhou, Zhuowen Tu, and Li Erran Li. Affordancellm: Grounding affordance from vision language models. In *Proceedings of the Second Workshop on Open-Vocabulary 3D Scene Understanding*, 2024.

Navid Rajabi and Jana Kosecka. Towards grounded visual spatial reasoning in multi-modal vision language models. In *ICLR 2024 Workshop on Data-centric Machine Learning Research (DMLR): Harnessing Momentum for Science*, 2024.

Hanoona Rasheed, Muhammad Maaz, Sahal Shaji, Abdelrahman Shaker, Salman Khan, Hisham Cholakkal, Rao M Anwer, Erix Xing, Ming-Hsuan Yang, and Fahad S Khan. Glamm: Pixel grounding large multimodal model. In *Proceedings of the IEEE/CVF Conference on Computer Vision and Pattern Recognition*, 2024.

Terry Regier and Laura A Carlson. Grounding spatial language in perception: an empirical and computational investigation. *Journal of experimental psychology: General*, 130(2):273, 2001.

Machel Reid, Nikolay Savinov, Denis Teplyashin, Dmitry Lepikhin, Timothy Lillicrap, Jean-baptiste Alayrac, Radu Soricut, Angeliki Lazaridou, Orhan Firat, Julian Schrittwieser, et al. Gemini 1.5: Unlocking multimodal understanding across millions of tokens of context. *arXiv preprint arXiv:2403.05530*, 2024.

David Romero, Chenyang Lyu, Haryo Akbarianto Wibowo, Teresa Lynn, Injy Hamed, Aditya Nanda Kishore, Aishik Mandal, Alina Dragonetti, Artem Abzaliev, Atnafu Lambebo Tonja, et al. Cvqa: Culturally-diverse multilingual visual question answering benchmark. *arXiv preprint arXiv:2406.05967*, 2024.

Michael Saxon, Ari Holtzman, Peter West, William Yang Wang, and Naomi Saphra. Benchmarks as microscopes: A call for model metrology. In *Proceedings of the First Conference on Language Modeling*, 2024.

Freda Shi, Mirac Suzgun, Markus Freitag, Xuezhi Wang, Suraj Srivats, Soroush Vosoughi, Hyung Won Chung, Yi Tay, Sebastian Ruder, Denny Zhou, et al. Language models are multilingual chain-of-thought reasoners. In *The Eleventh International Conference on Learning Representations*, 2023.

Anna Shusterman and Peggy Li. Frames of reference in spatial language acquisition. *Cognitive psychology*, 88:115–161, 2016.

Thora Tenbrink. Identifying objects on the basis of spatial contrast: An empirical study. In *International Conference on Spatial Cognition*, pp. 124–146. Springer, 2004.

Luca Tommasi and Bruno Laeng. Psychology of spatial cognition. *Wiley Interdisciplinary Reviews: Cognitive Science*, 3(6):565–580, 2012.

Maria Tsimpoukelli, Jacob L Menick, Serkan Cabi, SM Eslami, Oriol Vinyals, and Felix Hill. Multimodal few-shot learning with frozen language models. In *Advances in Neural Information Processing Systems*, volume 34, pp. 200–212, 2021.

Marina Vasilyeva and Stella F Lourenco. Development of spatial cognition. *Wiley Interdisciplinary Reviews: Cognitive Science*, 3(3):349–362, 2012.

Alex Warstadt and Samuel R Bowman. What artificial neural networks can tell us about human language acquisition. In *Algebraic structures in natural language*, pp. 17–60. CRC Press, 2022.

Zhuofan Xia, Dongchen Han, Yizeng Han, Xuran Pan, Shiji Song, and Gao Huang. Gsva: Generalized segmentation via multimodal large language models. In *Proceedings of the IEEE/CVF Conference on Computer Vision and Pattern Recognition*, 2024.

Jianing Yang, Xuweiyi Chen, Nikhil Madaan, Madhavan Iyengar, Shengyi Qian, David F Fouhey, and Joyce Chai. 3d-grand: A million-scale dataset for 3d-llms with better grounding and less hallucination. *arXiv preprint arXiv:2406.05132*, 2024.

Haoxuan You, Haotian Zhang, Zhe Gan, Xianzhi Du, Bowen Zhang, Zirui Wang, Liangliang Cao, Shih-Fu Chang, and Yinfei Yang. Ferret: Refer and ground anything anywhere at any granularity. In *The Twelfth International Conference on Learning Representations*, 2023.

Shoubin Yu, Jaehong Yoon, and Mohit Bansal. Crema: Multimodal compositional video reasoning via efficient modular adaptation and fusion. *arXiv preprint arXiv:2402.05889*, 2024a.

Tianyu Yu, Haoye Zhang, Yuan Yao, Yunkai Dang, Da Chen, Xiaoman Lu, Ganqu Cui, Taiwen He, Zhiyuan Liu, Tat-Seng Chua, et al. Rlaif-v: Aligning mllms through open-source ai feedback for super gpt-4v trustworthiness. *arXiv preprint arXiv:2405.17220*, 2024b.

Xiang Yue, Yuansheng Ni, Kai Zhang, Tianyu Zheng, Ruoqi Liu, Ge Zhang, Samuel Stevens, Dongfu Jiang, Weiming Ren, Yuxuan Sun, et al. Mmmu: A massive multi-discipline multimodal understanding and reasoning benchmark for expert agi. In *Proceedings of the IEEE/CVF Conference on Computer Vision and Pattern Recognition*, pp. 9556–9567, 2024.

Yichi Zhang, Jiayi Pan, Yuchen Zhou, Rui Pan, and Joyce Chai. Grounding visual illusions in language: Do vision-language models perceive illusions like humans? In *Proceedings of the 2023 Conference on Empirical Methods in Natural Language Processing*, pp. 5718–5728, 2023.

Yichi Zhang, Ziqiao Ma, Xiaofeng Gao, Suhaila Shakiah, Qiaozi Gao, and Joyce Chai. Groundhog: Grounding large language models to holistic segmentation. In *Proceedings of the IEEE/CVF Conference on Computer Vision and Pattern Recognition*, 2024.

A DATASET AND METRIC DETAILS

A.1 DATASET CONFIGURATIONS

The entire data generation pipeline produces 720 English test cases in COMFORT-BALL, and 57.6k English test cases in COMFORT-CAR. For COMFORT-BALL: 1 object combination × 5 variants × 4 relations × 36 angles = 720 test cases. For COMFORT-CAR: 20 object combinations × 5 variants × 4 relations × 36 angles × 4 prompts = 57,600 test cases. The table below lists all possible variants and configurations for the dataset, and we describe our dataset configuration in detail as follows.

Test Case Setup	Possible Variants
Scene $\mathcal{S}$	COMFORT-BALL: **Relatum**: *red ball*; **Referent**: *blue ball*; 36 samples uniformly collected along a rotational path.
	COMFORT-CAR: **Relatum**: *basketball*; **Referent**: *horse*, *car*, *bench*, *laptop*, *rubber duck*, *chair*, *dog*, *sofa*, *bed*, *bicycle*; **Addressee**: woman; 36 samples uniformly collected along a rotational path.
Spatial Relation $\mathcal{R}$	*to the left of*, *to the right of*, *in front of*, *behind*
Frame of Reference $\mathcal{F}$	*egocentric relative*, *addressee-centered relative*, *object-centered intrinsic*
Language $\mathcal{L}$	See Table 10.

Table 6: A test case in COMFORT is defined as a 4-tuple in $\mathcal{S} \times \mathcal{R} \times (\mathcal{F} \cup \{\emptyset\}) \times \mathcal{L}$. This table enumerates all possible variants and configurations of the dataset.

A.2 LIST OF EVALUATED LANGUAGES

We started with 132 candidate languages supported by Google Translate API.[4] We removed 23 languages from our multilingual evaluation due to their failure to adhere to instructions for generating "yes" and "no" predictions, or because they did not pass the back-translation test for quality control: Aymara, Bambara, Croatian, Dhivehi, Dogri, Ewe, Guarani, Hmong, Kyrgyz, Luganda, Malayalam, Meiteilon (Manipuri), Mizo, Odia (Oriya), Punjabi, Quechua, Samoan, Tatar, Telugu, Tigrinya, Uyghur, Xhosa, Yoruba.

A.3 VISUALIZATIONS OF REGION PARSING ERROR

(a) $\varepsilon^{\text{hemi}} = 10.7$ (b) $\varepsilon^{\text{hemi}} = 24.7$ (c) $\varepsilon^{\text{hemi}} = 34.8$ (d) $\varepsilon^{\text{hemi}} = 47.2$ (e) $\varepsilon^{\text{hemi}} = 55.5$

(f) $\varepsilon^{\text{cos}} = 10.4$ (g) $\varepsilon^{\text{cos}} = 22.4$ (h) $\varepsilon^{\text{cos}} = 32.6$ (i) $\varepsilon^{\text{cos}} = 42.1$ (j) $\varepsilon^{\text{cos}} = 50.3$
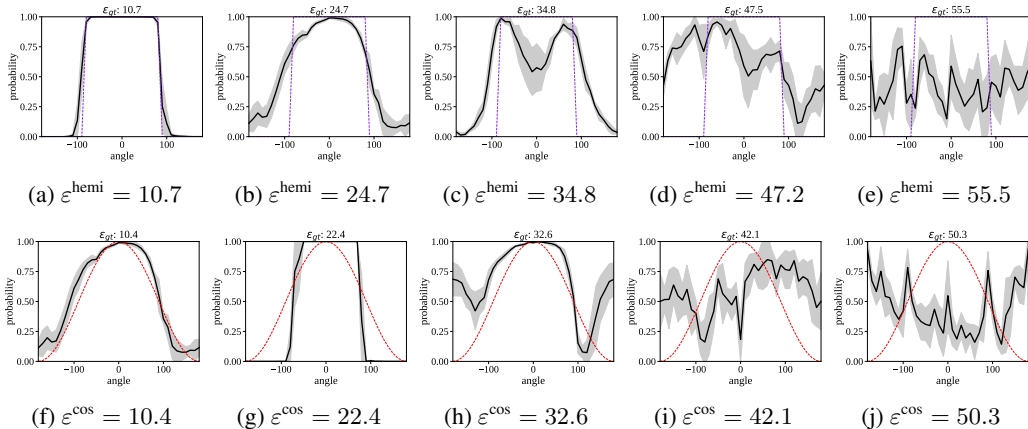
Figure 9: ε visualization: (a-e) correspond to $\varepsilon^{\text{hemi}}$, and (f-j) correspond to ε^{cos}.

B LIMITATIONS AND INTENDED USE

B.1 LIMITATIONS

The acceptance regions. Using cosine and hemisphere as acceptance regions is analytical but might not capture some human cognitive biases. In reality, regional angles might not be uniformly

---

[4]https://cloud.google.com/translate

distributed per relation, nor are they exactly 90 degrees. These angles vary across individuals and cultures (Franklin et al., 1995).

Spatial relations. This work primarily focuses on the most basic types of spatial relations (front-back and left-right). However, many other relations exist, such as *away from* and *near* (Logan & Sadler, 1996; Liu et al., 2023a). Additionally, not all languages possess terms for "left," "right," "front," and "back." Some languages, like Guugu Yimithirr, use only absolute frames of reference instead (Levinson, 2003).

Camera angle and occlusion. Currently, there is no occlusion, and the camera angle is high. Languages may differ in the importance placed on these factors, such as the preference to use "behind" in cases of occlusion (Levinson, 2003).

Pragmatic aspect of spatial cognition. Many conversational and pragmatic aspects of spatial cognition are simplified in this work, such as F-Formation (Kendon, 2010) and human-robot interaction (Liu et al., 2010). For example, in human-robot interaction settings, users prefer an addressee-centered frame of reference to facilitate the robot's comprehension of spatial referents (Moratz & Tenbrink, 2006).

Multilingual prompts. In this work, we used machine-translated text to construct the multilingual portion of the dataset. Although we verified data quality through back translation, incorporating human annotations in the future would be a valuable future step.

B.2 INTENDED USE

We intentionally use the term "framework" to emphasize that this dataset and its associated evaluation metrics are designed to assess cognitive similarity and alignment with human spatial cognition. While each studied language demonstrates a preference, we do not position this as a leaderboard-driven benchmark. However, the perspective-taking capability of VLMs as studied in § 4.3 can function as a benchmark, as the input and ground truth are unambiguous. We encourage future work in VLM training to address this specific challenge.

C CASE STUDIES

We added two case studies to augment the results in COMFORT:

C.1 ALTERNATIVE BACKGROUND

We first create a case study with a brown background color brown from COMFORT-BALL. We keep the objects visible and generate 36 images for each spatial relation. The images are shown below:
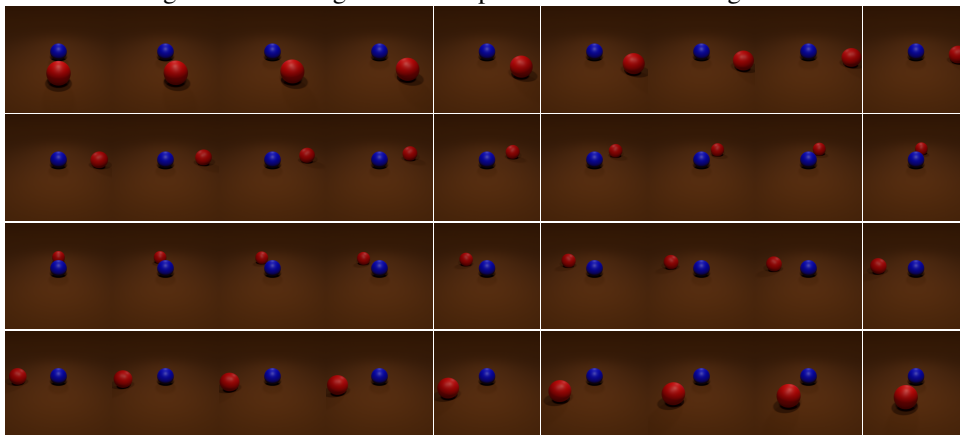
C.2 REAL-WORLD IMAGES

We added a pair of case studies to see if results in synthetic images generalize to real images. We first create a real-world version of the COMFORT-BALL dataset with no variations. We fixed the camera pose

and manually rotated the target object around the reference object using two equally sized red and blue balls, with all other setups identical to the Blender simulation. We took 36 images in total along the rotational path for each spatial relation. We also create a real-world version of the COMFORT-CAR dataset without the addressee. We used a laptop and the red ball to collect a set of 36 images for each spatial relation. The images are shown below:
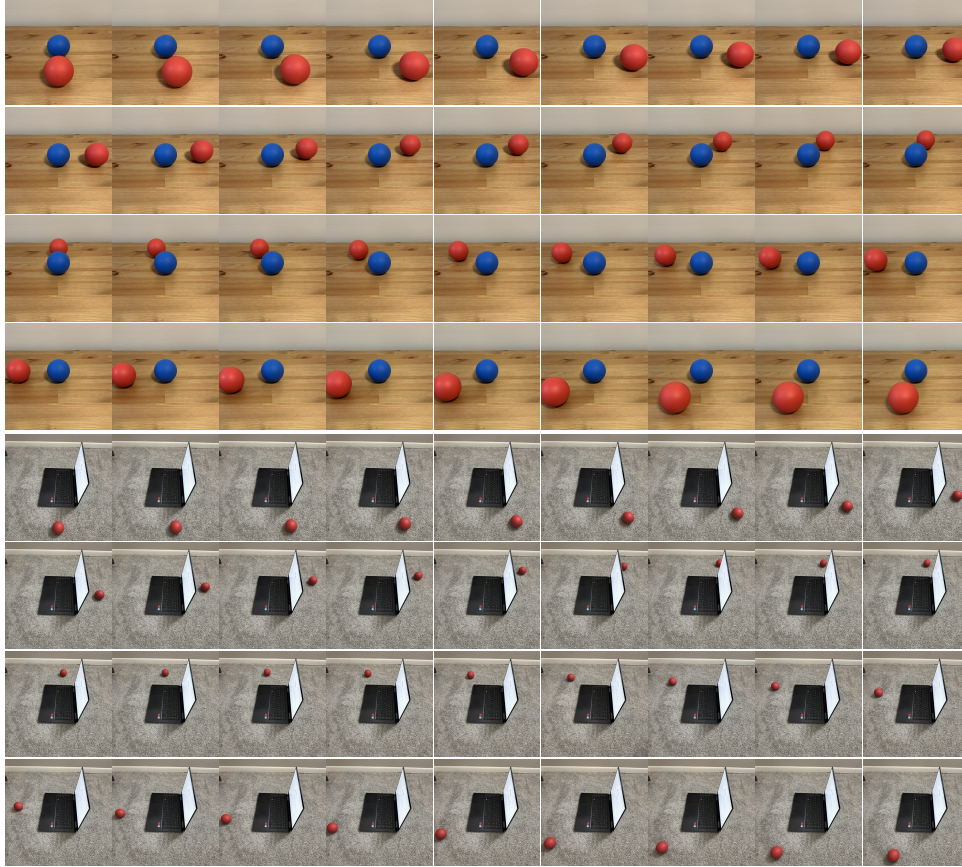
C.3 RESULTS

For the case study, we evaluated three VLMs: LLaVA-v1.5-7B/13B Liu et al. (2023b) and GPT-4o OpenAI (2024). Prediction plots under the camera perspective prompt (cam) are shown in Figure 10. Prediction plots under the camera perspective prompt (cam) are shown in Figure 11. Prediction plots under the camera perspective prompt (cam) are shown in Figure 12. Our findings remain consistent even when applied to these case studies and the general trend holds. However, we did observe that models performed with more noise compared to the synthetic data. We hypothesize that this noise arises from small inconsistencies between images in the real dataset, such as slight tilts in the positioning of the camera and the target object.

D ADDENDUM TO RESULTS
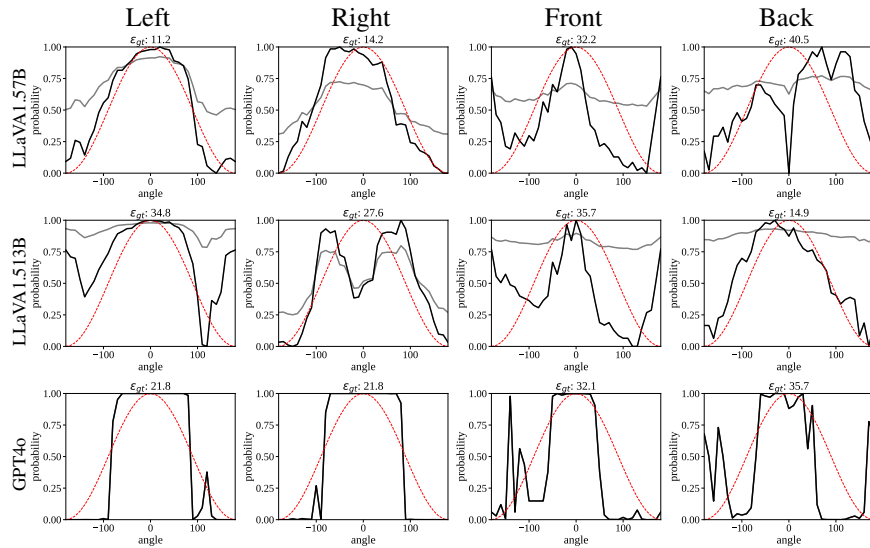
Figure 10: All prediction plots for each model on COMFORT-BALL with brown background using the camera perspective prompt (cam). The raw probability $p(\theta)$ in gray, normalized probability $\widehat{p}(\theta)$ in black, and the reference probability $p_{\cos}(\theta)$ of cam in red.
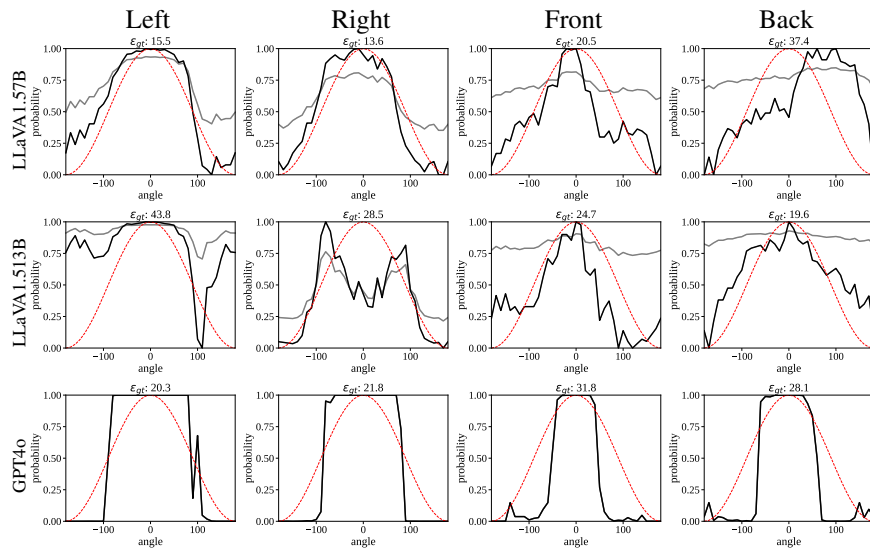
Figure 11: All prediction plots for each model on real image version of COMFORT-BALL using the camera perspective prompt (cam). The raw probability $p(\theta)$ in gray, normalized probability $\widehat{p}(\theta)$ in black, and the reference probability $p_{\cos}(\theta)$ of cam in red.
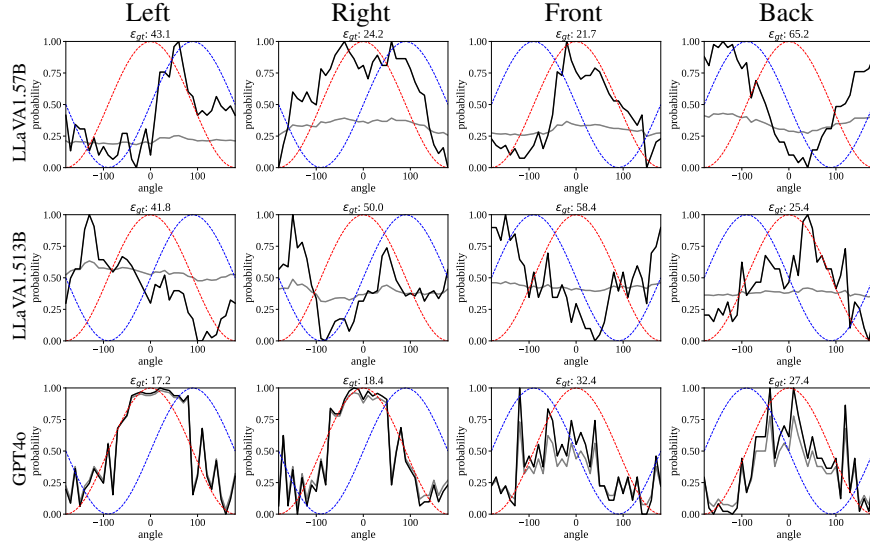
Figure 12: All prediction plots for each model on the real image version of `COMFORT-CAR` using the camera perspective prompt (`cam`). The raw probability $p(\theta)$ in gray, normalized probability $\widehat{p}(\theta)$ in black, and the reference probability $p_{\cos}(\theta)$ of `cam` in red, `rel` in blue.

| | Back | | | | | | Front | | | | | |
| | Same | | | Reversed | | | Same | | | Reversed | | |
	Acc%	$\varepsilon^{\text{hemi}}_{\times 10^2}$	$\varepsilon^{\text{cos}}_{\times 10^2}$	Acc%	$\varepsilon^{\text{hemi}}_{\times 10^2}$	$\varepsilon^{\text{cos}}_{\times 10^2}$	Acc%	$\varepsilon^{\text{hemi}}_{\times 10^2}$	$\varepsilon^{\text{cos}}_{\times 10^2}$	Acc%	$\varepsilon^{\text{hemi}}_{\times 10^2}$	$\varepsilon^{\text{cos}}_{\times 10^2}$
InstructBLIP-7B	47.2	58.4	45.6	47.2	53.8	39.0	47.2	47.5	31.6	47.2	64.6	52.0
InstructBLIP-13B	47.2	55.9	40.9	47.2	56.6	45.5	47.2	60.0	46.0	47.2	53.0	37.4
mBLIP	56.1	60.2	51.2	47.2	64.8	53.7	51.1	61.4	51.2	47.8	58.0	47.9
GLaMM	47.2	71.1	58.3	47.2	46.3	33.3	47.2	55.4	43.9	47.2	55.9	42.9
LLaVA-1.5-7B	47.2	66.7	54.0	47.2	47.0	32.9	47.2	71.0	59.1	47.2	36.4	24.8
LLaVA-1.5-13B	47.2	73.8	61.8	47.2	36.3	19.2	42.8	67.3	56.0	51.7	39.1	27.7
XComposer2	13.3	84.5	73.2	90.0	26.3	17.9	15.0	85.8	74.5	85.0	31.6	20.7
MiniCPM-V	13.9	84.1	70.9	80.6	35.6	21.9	26.1	77.0	64.3	75.0	35.3	26.9
GPT-4o	16.7	87.3	75.7	87.8	30.3	28.2	25.6	82.4	73.6	80.0	40.2	32.0

| | Left | | | | | | Right | | | | | |
| | Same | | | Reversed | | | Same | | | Reversed | | |
	Acc%	$\varepsilon^{\text{hemi}}_{\times 10^2}$	$\varepsilon^{\text{cos}}_{\times 10^2}$	Acc%	$\varepsilon^{\text{hemi}}_{\times 10^2}$	$\varepsilon^{\text{cos}}_{\times 10^2}$	Acc%	$\varepsilon^{\text{hemi}}_{\times 10^2}$	$\varepsilon^{\text{cos}}_{\times 10^2}$	Acc%	$\varepsilon^{\text{hemi}}_{\times 10^2}$	$\varepsilon^{\text{cos}}_{\times 10^2}$
InstructBLIP-7B	47.2	51.5	37.2	47.2	61.6	48.0	47.2	61.4	47.5	47.2	52.0	37.8
InstructBLIP-13B	47.2	54.2	43.4	47.2	57.0	44.9	47.2	58.1	45.6	47.2	52.5	41.6
mBLIP	47.2	59.8	52.4	47.2	64.2	53.5	47.8	65.7	54.6	47.8	56.4	46.8
GLaMM	47.2	48.9	38.3	47.2	65.5	51.8	79.4	29.8	17.3	15.0	76.2	63.7
LLaVA-1.5-7B	47.2	25.3	11.9	47.2	83.4	70.0	47.2	26.0	13.0	47.2	80.9	68.5
LLaVA-1.5-13B	62.8	39.1	31.7	31.7	76.8	61.8	91.1	35.8	24.3	8.9	79.3	64.3
XComposer2	97.8	11.3	20.1	3.3	95.6	80.9	96.7	15.2	21.3	3.3	95.8	81.1
MiniCPM-V	86.1	27.7	19.7	9.4	88.1	74.1	82.2	32.7	21.1	12.2	87.0	73.3
GPT-4o	94.4	20.4	24.3	11.1	92.6	80.8	94.4	19.0	25.1	11.1	92.8	80.8

| | Aggregated | | | | | | | | | |
| | Translated | | | Rotated | | | Reflected | | | Preferred Transform |
	Acc%	$\varepsilon^{\text{hemi}}_{\times 10^2}$	$\varepsilon^{\text{cos}}_{\times 10^2}$	Acc%	$\varepsilon^{\text{hemi}}_{\times 10^2}$	$\varepsilon^{\text{cos}}_{\times 10^2}$	Acc%	$\varepsilon^{\text{hemi}}_{\times 10^2}$	$\varepsilon^{\text{cos}}_{\times 10^2}$	
InstructBLIP-7B	47.2	54.7	40.5	47.2	58.0	44.2	47.2	57.8	43.9	Not Significant
InstructBLIP-13B	47.2	57.1	44.0	47.2	54.8	42.3	47.2	55.5	43.0	Not Significant
mBLIP	50.6	61.8	52.3	47.5	60.9	50.5	47.5	62.1	52.1	Not Significant
GLaMM	55.3	51.3	39.5	39.2	61.0	47.9	55.3	45.2	33.0	Reflected
LLaVA-1.5-7B	47.2	47.3	34.5	47.2	61.9	49.0	47.2	33.7	20.7	Reflected
LLaVA-1.5-13B	61.0	54.0	43.4	34.9	57.9	43.2	63.2	37.6	25.7	Reflected
XComposer2	55.7	49.2	47.3	45.4	62.3	50.1	92.4	21.1	20.0	Reflected
MiniCPM-V	52.1	55.4	44.0	44.3	61.5	49.1	81.0	32.8	22.4	Reflected
GPT-4o	57.8	52.3	49.7	47.5	64.0	55.5	89.2	27.5	27.4	Reflected

Table 7: The full results for testing the preferred coordinate transformation mapping from the viewer to the relatum in the relative frame of reference.

| | Back | | | | | | | | | Front | | | | | | | | |
| | Egocentric | | | Intrinsic | | | Addressee | | | Egocentric | | | Intrinsic | | | Addressee | | |
	Acc%	$\varepsilon^{hemi}_{\times10^2}$	$\varepsilon^{cos}_{\times10^2}$	Acc%	$\varepsilon^{hemi}_{\times10^2}$	$\varepsilon^{cos}_{\times10^2}$	Acc%	$\varepsilon^{hemi}_{\times10^2}$	$\varepsilon^{cos}_{\times10^2}$	Acc%	$\varepsilon^{hemi}_{\times10^2}$	$\varepsilon^{cos}_{\times10^2}$	Acc%	$\varepsilon^{hemi}_{\times10^2}$	$\varepsilon^{cos}_{\times10^2}$	Acc%	$\varepsilon^{hemi}_{\times10^2}$	$\varepsilon^{cos}_{\times10^2}$
InstructBLIP-7B	47.2	51.4	41.0	47.2	53.0	38.6	47.2	53.0	38.6	47.2	54.2	40.9	47.2	60.7	46.9	47.2	60.7	46.9
InstructBLIP-13B	47.2	43.5	32.9	47.2	48.9	34.4	47.2	48.9	34.4	47.2	66.5	52.5	47.2	61.1	48.5	47.2	61.1	48.5
mBLIP-BLOOMZ	52.8	62.1	52.2	52.8	63.9	53.2	52.8	63.9	53.2	52.8	56.4	45.3	52.8	55.5	44.6	52.8	55.5	44.6
GLaMM	47.2	45.6	31.9	47.2	51.0	38.8	47.2	51.0	38.8	47.2	37.9	24.8	47.2	69.6	57.1	47.2	69.6	57.1
LLaVA-1.5-7B	49.2	41.6	28.0	47.5	60.3	49.1	47.5	60.3	49.1	48.6	43.2	30.0	48.6	52.9	40.2	48.6	52.9	40.2
LLaVA-1.5-13B	50.8	36.8	20.9	48.6	54.7	43.0	48.6	54.7	43.0	47.2	46.5	34.5	47.2	47.3	32.6	47.2	47.3	32.6
XComposer2	91.4	25.0	12.7	53.6	59.9	49.3	53.6	59.9	49.3	87.8	26.6	15.2	55.0	59.3	48.3	55.0	59.3	48.3
MiniCPM-V	66.4	46.5	34.2	60.8	51.3	40.7	60.8	51.3	40.7	57.5	45.0	35.5	50.8	64.6	53.4	50.8	64.6	53.4
GPT-4o	64.2	49.1	38.3	66.4	45.4	36.7	66.4	45.4	36.7	58.1	54.8	43.1	53.6	61.0	50.2	53.6	61.0	50.2

| | Left | | | | | | | | | Right | | | | | | | | |
| | Egocentric | | | Intrinsic | | | Addressee | | | Egocentric | | | Intrinsic | | | Addressee | | |
	Acc%	$\varepsilon^{hemi}_{\times10^2}$	$\varepsilon^{cos}_{\times10^2}$	Acc%	$\varepsilon^{hemi}_{\times10^2}$	$\varepsilon^{cos}_{\times10^2}$	Acc%	$\varepsilon^{hemi}_{\times10^2}$	$\varepsilon^{cos}_{\times10^2}$	Acc%	$\varepsilon^{hemi}_{\times10^2}$	$\varepsilon^{cos}_{\times10^2}$	Acc%	$\varepsilon^{hemi}_{\times10^2}$	$\varepsilon^{cos}_{\times10^2}$	Acc%	$\varepsilon^{hemi}_{\times10^2}$	$\varepsilon^{cos}_{\times10^2}$
InstructBLIP-7B	47.2	59.0	45.6	47.2	45.3	32.5	47.2	62.0	51.9	47.2	53.1	39.6	47.2	61.7	51.2	47.2	45.3	31.8
InstructBLIP-13B	47.2	59.7	47.8	47.2	70.2	56.2	47.2	39.6	27.8	47.2	53.6	40.6	47.2	39.5	27.6	47.2	70.8	56.6
mBLIP-BLOOMZ	52.8	58.2	47.8	52.8	59.7	47.6	52.8	58.4	48.1	52.8	57.7	45.4	52.8	60.6	48.4	52.8	53.8	42.4
GLaMM	75.8	22.3	11.7	46.4	62.0	51.1	52.5	62.3	51.1	60.8	41.8	27.5	44.7	68.5	57.4	53.1	58.7	48.7
LLaVA-1.5-7B	76.7	25.6	14.0	33.9	68.2	56.8	64.4	52.7	41.5	56.4	28.5	13.7	44.2	64.6	53.0	52.5	57.3	46.6
LLaVA-1.5-13B	81.7	23.7	13.4	42.2	65.0	53.5	57.2	58.5	47.4	86.7	26.8	14.3	47.8	64.0	53.6	52.2	59.9	49.3
XComposer2	95.0	18.8	18.8	45.6	70.5	61.2	54.4	64.0	53.7	96.1	17.1	16.5	47.8	68.1	58.4	52.2	64.6	54.5
MiniCPM-V	93.3	20.4	18.0	52.2	64.3	53.9	47.8	68.0	58.4	91.7	22.6	19.0	46.1	68.3	58.1	53.9	62.5	52.7
GPT-4o	78.6	42.1	34.7	48.1	69.4	59.3	51.9	65.8	56.5	93.9	21.8	24.3	52.8	67.0	57.3	47.2	71.0	61.7

| | Aggregated | | | | | | | | | |
| | Egocentric | | | Intrinsic | | | Addressee | | | Preferred FoR |
	Acc%	$\varepsilon^{hemi}_{\times10^2}$	$\varepsilon^{cos}_{\times10^2}$	Acc%	$\varepsilon^{hemi}_{\times10^2}$	$\varepsilon^{cos}_{\times10^2}$	Acc%	$\varepsilon^{hemi}_{\times10^2}$	$\varepsilon^{cos}_{\times10^2}$	
InstructBLIP-7B	47.2	54.4	41.8	47.2	55.2	42.3	47.2	55.2	42.3	Not Significant
InstructBLIP-13B	47.2	55.8	43.5	47.2	54.9	41.7	47.2	55.1	41.8	Not Significant
mBLIP-BLOOMZ	52.8	58.6	47.7	52.8	59.9	48.4	52.8	57.9	47.1	Not Significant
GLaMM	57.8	36.9	24.0	46.4	62.8	51.1	50.0	60.4	48.9	Egocentric Relative
LLaVA-1.5-7B	57.7	34.7	21.4	43.5	61.5	49.8	53.3	55.8	44.4	Egocentric Relative
LLaVA-1.5-13B	66.6	33.5	20.8	46.5	57.7	45.7	51.3	55.1	43.1	Egocentric Relative
XComposer2	92.6	21.9	15.8	50.5	64.4	54.3	53.8	61.9	51.4	Egocentric Relative
MiniCPM-V	77.2	33.7	26.7	52.5	62.1	51.5	53.3	61.6	51.3	Egocentric Relative
GPT-4o	73.7	42.0	35.1	55.2	60.7	50.9	54.8	60.8	51.3	Egocentric Relative

Table 8: The full results for testing the preferred frame of reference in VLMs.

| | Back | | | | | | | | | Front | | | | | | | | |
| | Egocentric | | | Intrinsic | | | Addressee | | | Egocentric | | | Intrinsic | | | Addressee | | |
	Acc%	$\varepsilon^{hemi}_{\times10^2}$	$\varepsilon^{cos}_{\times10^2}$	Acc%	$\varepsilon^{hemi}_{\times10^2}$	$\varepsilon^{cos}_{\times10^2}$	Acc%	$\varepsilon^{hemi}_{\times10^2}$	$\varepsilon^{cos}_{\times10^2}$	Acc%	$\varepsilon^{hemi}_{\times10^2}$	$\varepsilon^{cos}_{\times10^2}$	Acc%	$\varepsilon^{hemi}_{\times10^2}$	$\varepsilon^{cos}_{\times10^2}$	Acc%	$\varepsilon^{hemi}_{\times10^2}$	$\varepsilon^{cos}_{\times10^2}$
InstructBLIP-7B	47.2	56.4	45.1	47.2	54.3	41.2	47.2	56.0	42.8	47.2	56.2	42.0	47.2	56.4	43.6	47.2	56.3	43.3
InstructBLIP-13B	47.2	49.2	38.1	47.2	54.0	40.4	47.2	53.8	40.9	47.2	63.0	49.8	47.2	58.6	46.2	47.2	59.7	47.6
mBLIP-BLOOMZ	52.9	65.4	55.3	52.4	64.7	54.8	50.8	66.3	57.1	52.6	66.2	56.3	52.1	63.8	52.8	53.1	67.1	58.9
GLaMM	47.2	46.2	32.7	47.2	54.8	42.4	47.2	62.6	49.9	47.2	40.4	25.3	47.2	55.1	41.6	47.2	51.0	38.3
LLaVA-1.5-7B	49.0	41.6	27.6	47.4	56.3	45.7	46.2	66.7	55.0	47.5	39.4	25.2	47.4	52.9	39.8	47.2	41.1	27.5
LLaVA-1.5-13B	47.2	38.3	22.4	47.2	53.2	41.1	47.2	52.1	39.9	47.2	48.8	36.8	47.2	54.7	41.2	47.2	41.9	26.8
XComposer2	65.4	40.6	26.0	52.2	57.9	47.0	54.0	58.5	47.5	86.9	27.0	17.1	52.1	58.9	47.8	53.1	57.8	46.6
MiniCPM-V	55.7	48.6	36.0	46.9	57.7	45.9	53.8	47.4	36.3	54.7	45.9	35.0	52.2	58.4	45.9	52.2	58.5	46.9
GPT-4o	69.0	41.3	28.7	59.7	50.0	37.7	56.4	48.7	36.0	58.6	52.5	40.3	52.1	57.4	45.1	48.3	60.0	46.9

| | Left | | | | | | | | | Right | | | | | | | | |
| | Egocentric | | | Intrinsic | | | Addressee | | | Egocentric | | | Intrinsic | | | Addressee | | |
	Acc%	$\varepsilon^{hemi}_{\times10^2}$	$\varepsilon^{cos}_{\times10^2}$	Acc%	$\varepsilon^{hemi}_{\times10^2}$	$\varepsilon^{cos}_{\times10^2}$	Acc%	$\varepsilon^{hemi}_{\times10^2}$	$\varepsilon^{cos}_{\times10^2}$	Acc%	$\varepsilon^{hemi}_{\times10^2}$	$\varepsilon^{cos}_{\times10^2}$	Acc%	$\varepsilon^{hemi}_{\times10^2}$	$\varepsilon^{cos}_{\times10^2}$	Acc%	$\varepsilon^{hemi}_{\times10^2}$	$\varepsilon^{cos}_{\times10^2}$
InstructBLIP-7B	47.2	56.3	43.3	47.2	56.0	43.0	47.2	57.9	47.1	47.2	56.8	43.5	47.2	52.9	41.5	47.2	54.4	41.0
InstructBLIP-13B	47.2	58.0	46.2	47.2	61.7	48.7	47.2	46.5	33.8	47.2	53.5	41.1	47.2	49.8	37.6	47.2	62.6	49.4
mBLIP-BLOOMZ	51.4	65.6	55.4	46.4	67.0	56.4	47.2	64.6	54.8	50.7	65.3	54.4	48.2	63.5	52.8	47.2	62.9	52.3
GLaMM	47.2	29.6	16.9	47.2	57.7	45.8	47.2	53.7	41.5	47.2	34.3	18.3	47.2	58.7	47.1	47.2	53.2	41.6
LLaVA-1.5-7B	64.9	23.7	12.1	50.4	60.2	48.9	49.9	56.3	45.3	59.3	25.2	8.7	47.9	59.8	48.5	49.6	56.7	45.7
LLaVA-1.5-13B	47.2	29.2	18.3	47.2	59.5	47.0	47.2	53.5	41.2	64.7	32.1	17.9	47.4	61.6	50.7	48.5	58.6	47.8
XComposer2	95.6	18.4	16.4	49.7	64.8	54.5	54.0	62.1	51.8	94.4	19.2	15.7	49.9	64.9	54.8	51.8	64.3	53.8
MiniCPM-V	89.4	24.2	13.3	50.4	60.9	50.0	52.1	60.6	49.9	89.9	24.3	14.2	50.1	60.6	49.5	53.3	58.0	47.3
GPT-4o	91.7	24.0	22.8	52.5	60.1	48.6	46.7	59.9	47.6	93.9	22.1	20.5	49.2	59.4	47.0	45.1	61.0	49.1

Table 9: The full results for benchmarking perspective-taking performance in VLMs.

Code	Language	Intrinsic	Egocentric Ref.	Rot.	Tran.	Addressee Ref.	Rot.	Tran.	Code	Language	Intrinsic	Egocentric Ref.	Rot.	Tran.	Addressee Ref.	Rot.	Tran.
af	Afrikaans	50.9	33.7	57.8	49.2	56.6	55.5	57.5	ku	Kurdish	56.5	49.5	54.4	53.1	53.1	55.2	54.0
ak	Akan	51.8	39.6	52.2	48.8	50.4	50.6	53.8	la	Latin	52.2	43.9	49.8	55.5	55.1	50.8	56.6
am	Amharic	52.1	47.4	60.7	50.9	56.8	54.2	57.6	lb	Luxembourgish	54.7	35.6	57.6	50.3	58.6	53.0	59.9
ar	Arabic	55.7	35.8	59.0	51.0	56.6	55.8	59.8	ln	Lingala	52.6	45.7	50.3	59.4	54.6	51.3	58.0
as	Assamese	51.6	40.8	55.3	51.6	48.8	52.8	56.0	lo	Lao	55.8	40.1	55.0	53.7	54.7	55.7	55.5
az	Azerbaijani	49.8	41.9	56.2	51.6	50.7	52.4	55.5	lt	Lithuanian	54.4	35.5	58.3	51.6	57.4	56.5	59.1
be	Belarusian	54.4	39.7	61.7	46.5	51.1	51.9	58.9	lv	Latvian	55.8	35.5	57.7	53.8	57.9	58.7	58.8
bg	Bulgarian	56.9	32.8	56.0	51.4	55.7	55.6	58.9	mai	Maithili	52.7	39.8	55.1	49.9	51.2	50.6	56.5
bho	Bhojpuri	51.5	42.8	58.3	47.5	52.3	51.4	56.5	mg	Malagasy	47.1	37.1	52.2	48.1	53.1	50.9	53.5
bn	Bengali	55.8	34.5	57.1	50.2	53.8	56.1	57.4	mi	Maori	52.0	36.6	58.5	47.6	52.0	51.9	58.1
bs	Bosnian	55.1	35.2	58.5	49.6	54.3	53.1	59.4	mk	Macedonian	54.8	37.0	59.1	49.5	56.5	56.0	58.1
ca	Catalan	55.6	34.7	56.9	53.0	56.0	56.4	59.7	mn	Mongolian	54.1	36.7	56.8	47.4	54.7	53.6	54.7
ceb	Cebuano	52.9	40.0	52.7	54.9	55.3	49.5	60.3	mr	Marathi	52.9	34.5	55.0	48.3	51.7	52.4	55.4
ckb	Sorani	50.4	36.1	53.3	50.6	50.3	52.0	56.3	ms	Malay	54.2	33.1	55.8	50.5	55.9	55.4	57.9
co	Corsican	57.6	35.4	57.4	54.3	58.8	58.8	59.7	mt	Maltese	53.4	37.5	56.1	49.2	50.8	53.8	55.5
cs	Czech	56.4	35.7	58.2	52.4	57.0	58.5	58.0	my	Myanmar	54.9	39.3	58.7	51.8	54.2	56.1	58.1
cy	Welsh	55.1	36.7	59.5	48.7	54.9	54.8	58.5	nb	Norwegian	55.1	34.7	57.0	52.1	58.1	57.6	57.3
da	Danish	54.9	33.0	55.2	53.1	57.6	58.3	56.9	ne	Nepali	53.1	39.4	58.4	47.3	52.9	54.1	54.0
de	German	55.7	36.2	58.4	52.8	56.9	56.6	60.3	nl	Dutch	51.7	34.5	56.3	48.3	53.5	51.6	57.8
el	Greek	54.4	34.4	57.1	52.2	57.1	57.5	57.7	nso	Sepedi	53.8	42.6	51.0	57.1	46.3	54.2	53.7
en	English	50.9	35.8	57.3	53.7	58.8	51.3	58.8	ny	Nyanja	53.7	34.5	56.6	48.0	54.4	52.8	56.7
eo	Esperanto	58.0	34.3	56.4	54.6	58.2	58.2	60.2	om	Oromo	51.1	43.5	57.3	50.6	54.9	54.8	52.9
es	Spanish	56.9	36.2	58.1	53.3	57.0	58.5	59.0	pl	Polish	55.8	32.9	55.8	52.5	55.1	55.1	59.5
et	Estonian	53.7	35.1	56.0	51.7	55.0	54.8	58.5	ps	Pashto	53.0	34.6	57.4	48.9	53.7	54.6	57.4
eu	Basque	56.8	34.3	56.8	53.2	56.7	57.1	59.5	pt	Portuguese	56.3	35.9	58.2	51.9	59.1	59.3	57.6
fa	Persian	55.8	32.1	55.3	49.8	54.4	53.8	58.0	ro	Romanian	57.1	34.8	57.0	53.8	58.2	58.6	59.1
fi	Finnish	53.9	33.7	56.7	50.8	56.3	56.1	57.6	ru	Russian	56.2	36.9	58.8	53.0	56.8	56.3	60.8
fil	Filipino	50.9	31.1	54.1	49.2	54.3	54.0	55.7	rw	Kinyarwanda	53.2	35.2	56.7	48.9	54.4	54.1	57.2
fr	French	58.0	35.2	57.4	53.7	58.6	58.5	59.4	sa	Sanskrit	51.9	41.2	54.1	51.9	51.7	56.4	51.6
fy	Frisian	53.9	38.2	58.9	49.6	53.4	53.2	59.2	sd	Sindhi	51.3	40.3	56.5	49.1	54.8	49.8	57.4
ga	Irish	54.0	33.2	55.3	49.2	52.7	55.7	53.9	si	Sinhala	52.4	38.4	54.6	48.6	53.4	51.5	56.6
gd	Scots Gaelic	53.9	35.4	58.5	49.6	54.7	55.8	58.1	sk	Slovak	56.1	37.7	57.1	54.7	57.2	56.7	59.8
gl	Galician	56.6	37.1	59.0	53.4	57.9	57.9	60.0	sl	Slovenian	55.8	36.5	59.3	49.5	53.9	54.3	58.9
gom	Konkani	51.1	53.1	55.5	50.5	52.5	54.9	51.8	sn	Shona	56.0	34.7	56.0	52.2	54.8	55.6	58.5
gu	Gujarati	52.6	36.6	54.2	50.9	55.5	55.3	53.8	so	Somali	53.7	34.3	56.4	48.2	50.0	51.6	58.4
ha	Hausa	54.0	41.0	56.1	53.0	52.8	55.3	56.1	sq	Albanian	53.6	35.1	56.4	49.0	52.6	50.3	60.1
haw	Hawaiian	55.3	42.2	62.1	51.5	60.5	56.2	60.8	sr	Serbian	55.4	34.5	57.2	50.9	52.5	55.0	58.8
he	Hebrew	56.5	36.4	58.8	52.5	57.1	56.5	60.3	st	Sesotho	53.9	38.4	55.4	51.0	51.3	54.4	55.8
hi	Hindi	52.5	37.8	56.6	49.1	54.5	54.6	54.2	su	Sundanese	51.3	36.7	55.0	50.0	53.7	50.4	57.7
ht	Haitian Creole	56.1	36.0	58.3	53.6	58.4	58.2	59.6	sv	Swedish	54.0	33.5	56.7	51.7	55.8	56.3	58.2
hu	Hungarian	55.2	35.0	57.5	50.7	56.1	56.8	56.7	sw	Swahili	55.3	34.2	56.8	52.4	57.2	56.5	58.4
hy	Armenian	52.2	35.4	56.7	48.8	53.6	52.5	57.2	ta	Tamil	52.0	40.4	55.2	51.1	52.2	52.9	54.6
id	Indonesian	55.9	35.6	58.1	52.2	57.1	57.8	58.1	tg	Tajik	55.7	36.7	57.7	49.7	55.4	56.6	56.3
ig	Igbo	54.5	33.8	56.7	47.4	53.6	53.2	55.3	th	Thai	55.5	35.4	57.9	50.8	56.2	57.8	57.3
ilo	Ilocano	50.8	44.6	46.7	58.9	48.9	57.0	48.7	tk	Turkmen	52.3	45.3	59.0	51.5	52.6	51.2	59.1
is	Icelandic	55.9	34.2	57.0	52.2	56.5	58.0	57.3	tr	Turkish	55.3	33.6	56.3	50.8	56.2	57.0	56.3
it	Italian	56.8	35.6	57.6	53.6	57.9	58.2	59.6	ts	Tsonga	49.4	44.6	50.0	53.7	53.3	51.5	53.6
ja	Japanese	54.7	34.5	56.9	50.4	54.4	55.9	57.3	uk	Ukrainian	56.6	36.1	58.8	50.1	56.8	55.7	59.7
jv	Javanese	53.5	35.3	57.7	51.0	55.7	54.8	58.9	ur	Urdu	52.3	34.6	56.7	49.7	54.0	55.1	57.0
ka	Georgian	51.1	34.8	54.3	50.6	52.0	54.0	55.3	uz	Uzbek	52.6	34.5	56.4	48.1	51.7	53.2	56.6
kk	Kazakh	52.6	36.5	58.8	50.4	54.0	56.1	56.9	vi	Vietnamese	53.9	34.6	58.5	48.6	55.7	56.1	56.8
km	Khmer	55.6	37.6	60.2	50.5	56.9	56.6	59.3	yi	Yiddish	56.7	36.5	57.9	53.5	56.8	57.3	60.0
kn	Kannada	52.3	40.8	53.2	49.5	49.6	51.9	53.4	zh	Yoruba	54.6	35.5	58.3	51.4	56.9	57.2	57.8
ko	Korean	53.6	36.5	59.1	49.7	53.3	53.5	59.8	zu	Chinese	55.6	35.9	57.7	53.1	55.3	56.5	60.2
kri	Krio	58.3	36.2	57.1	51.2	56.1	53.2	60.2									

Table 10: The full results for the cross-lingual and cross-cultural evaluation of the preferred frame of reference in VLMs.
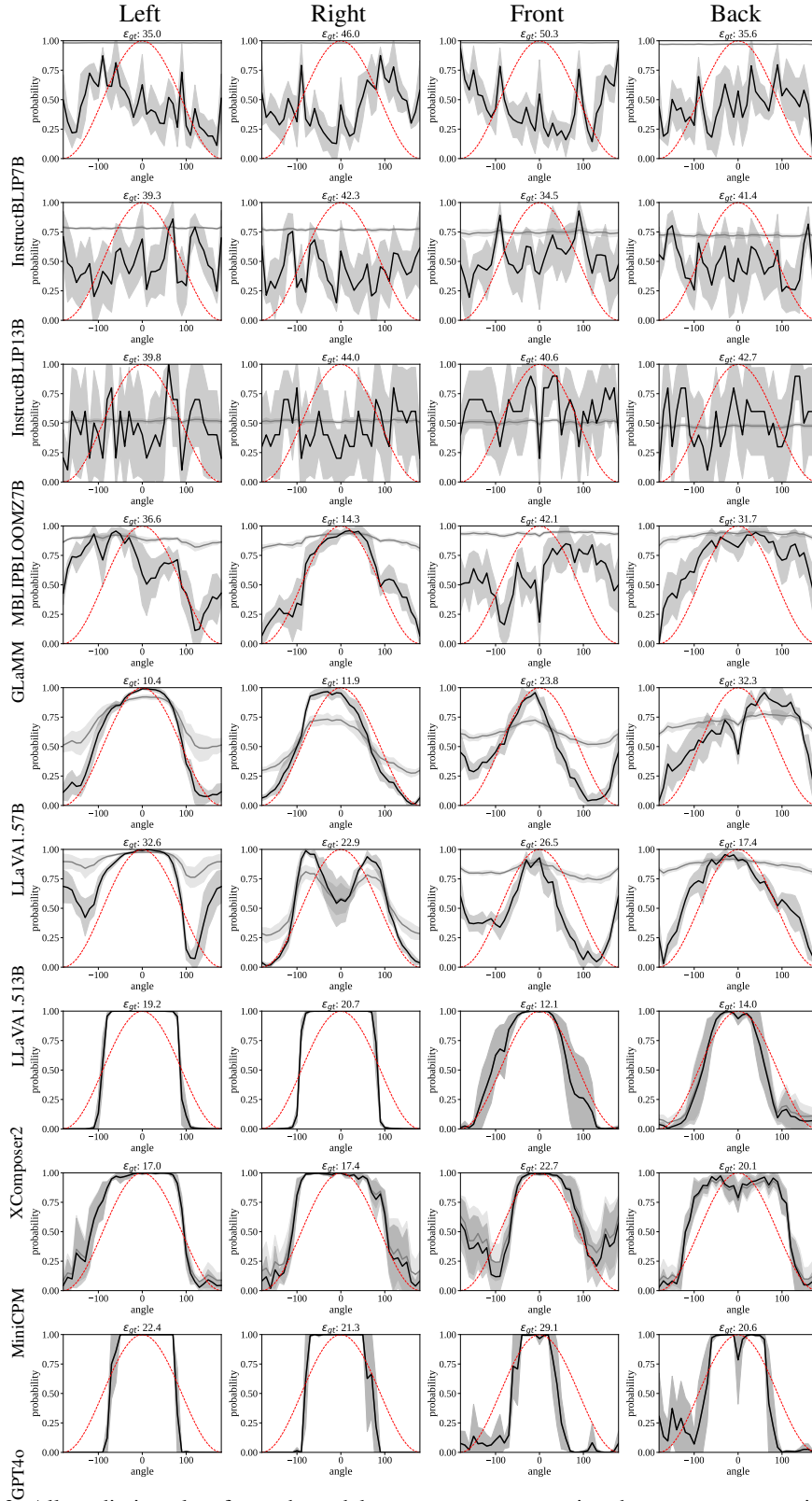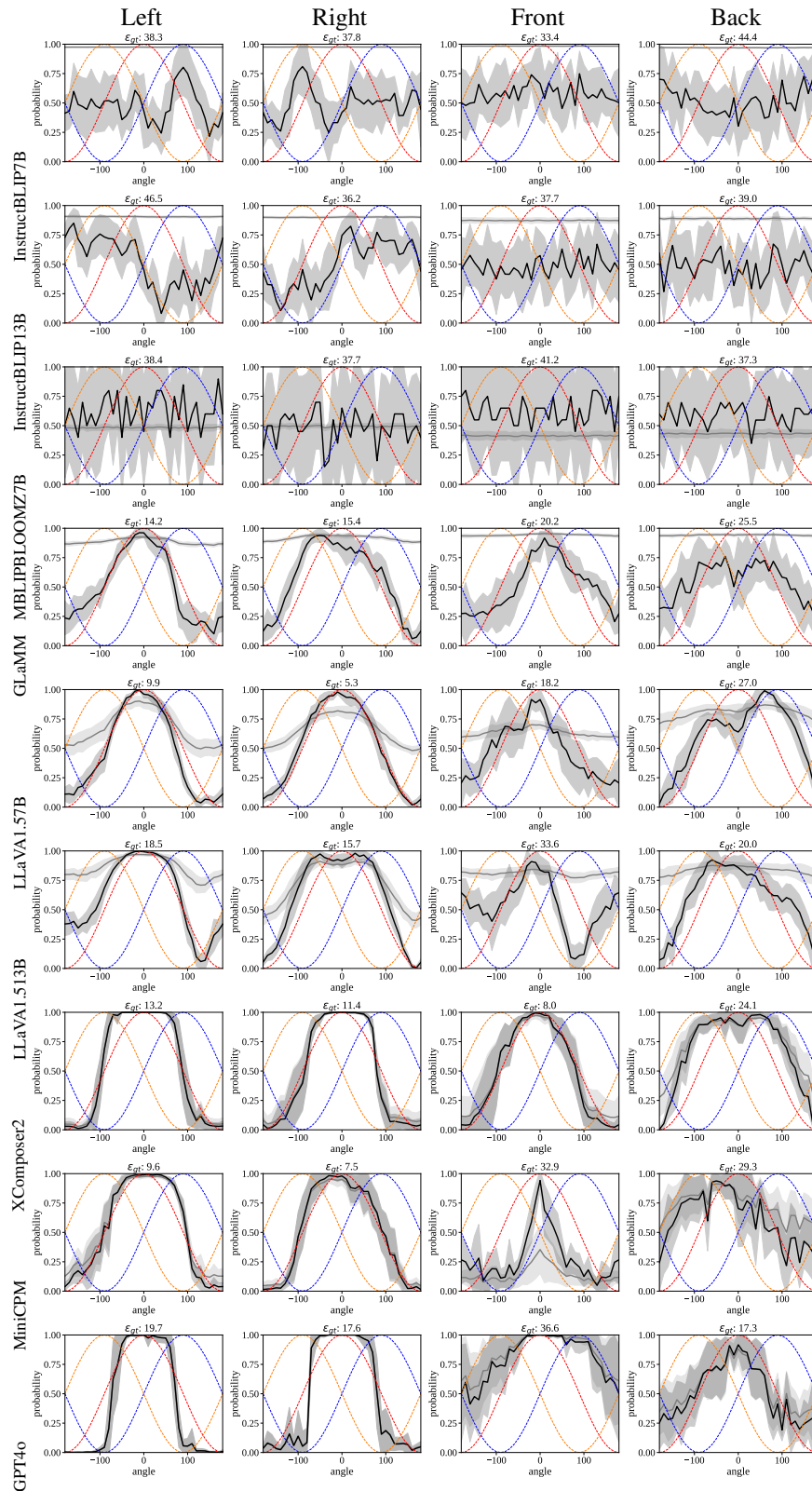
Figure 13: All prediction plots for each model on COMFORT-BALL using the camera perspective prompt (cam). The raw probability $p(\theta)$ in gray, normalized probability $\widehat{p}(\theta)$ in black, and the reference probability $p_{\cos}(\theta)$ of cam in red.

Figure 14: All prediction plots for each model on COMFORT-CAR using the camera perspective prompt (cam). The raw probability $p(\theta)$ in gray, normalized probability $\widehat{p}(\theta)$ in black, and the reference probabilities $p_{\cos}(\theta)$ of cam in red, add in orange, rel in blue. To avoid overlapping reference probabilities of add and rel, we use plots on COMFORT-CAR with relatum facing left for left and right relations and COMFORT-CAR with relatum facing right for front and behind relations.
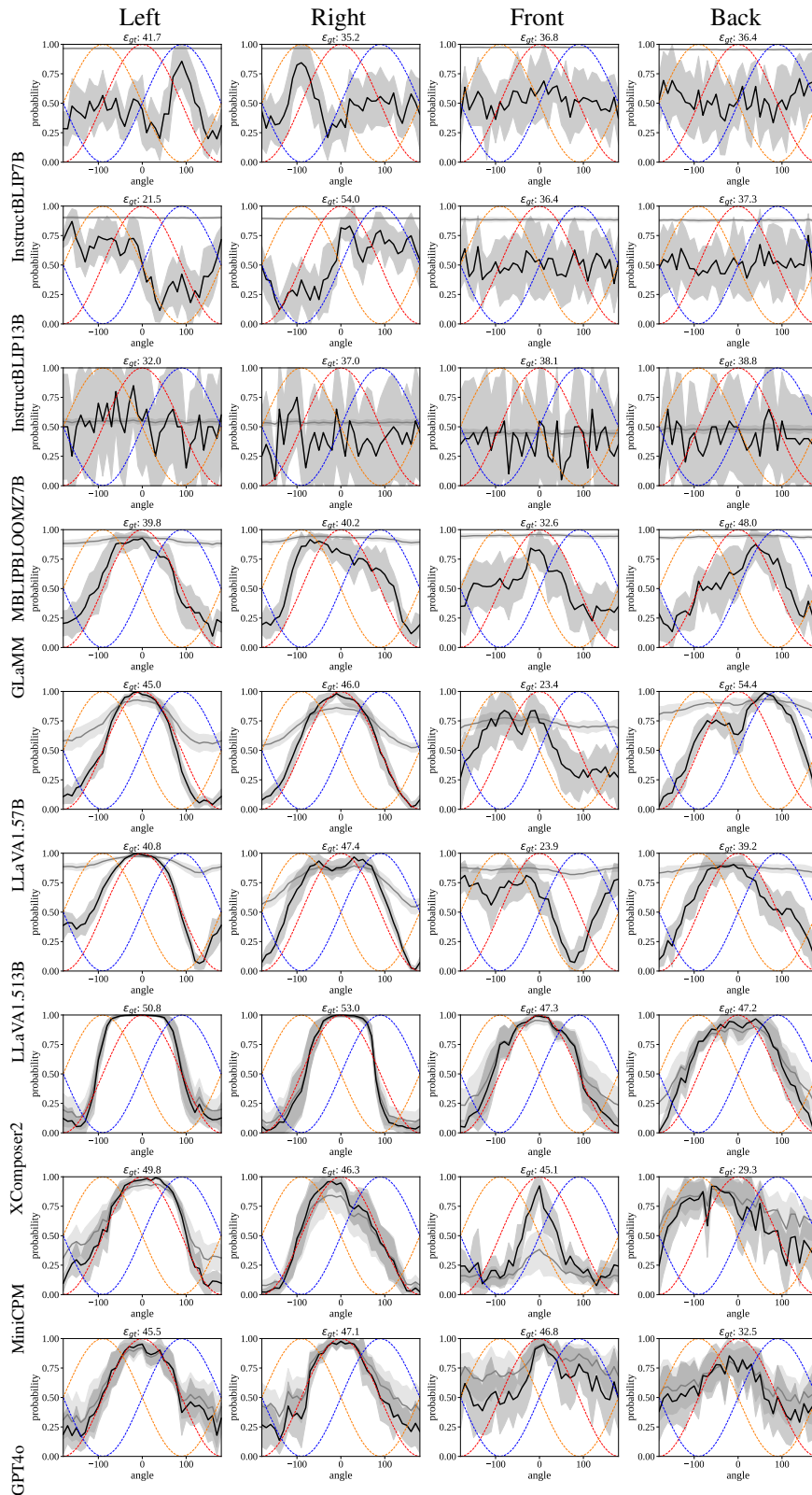
Figure 15: All prediction plots for each model on COMFORT-CAR using the addressee perspective prompt (add). The raw probability $p(\theta)$ in gray, normalized probability $\widehat{p}(\theta)$ in black, and the reference probabilities $p_{\cos}(\theta)$ of cam in red, add in orange, rel in blue. To avoid overlapping reference probabilities of add and rel, we use plots on COMFORT-CAR with relatum facing left for left and right relations and COMFORT-CAR with relatum facing right for front and behind relations.
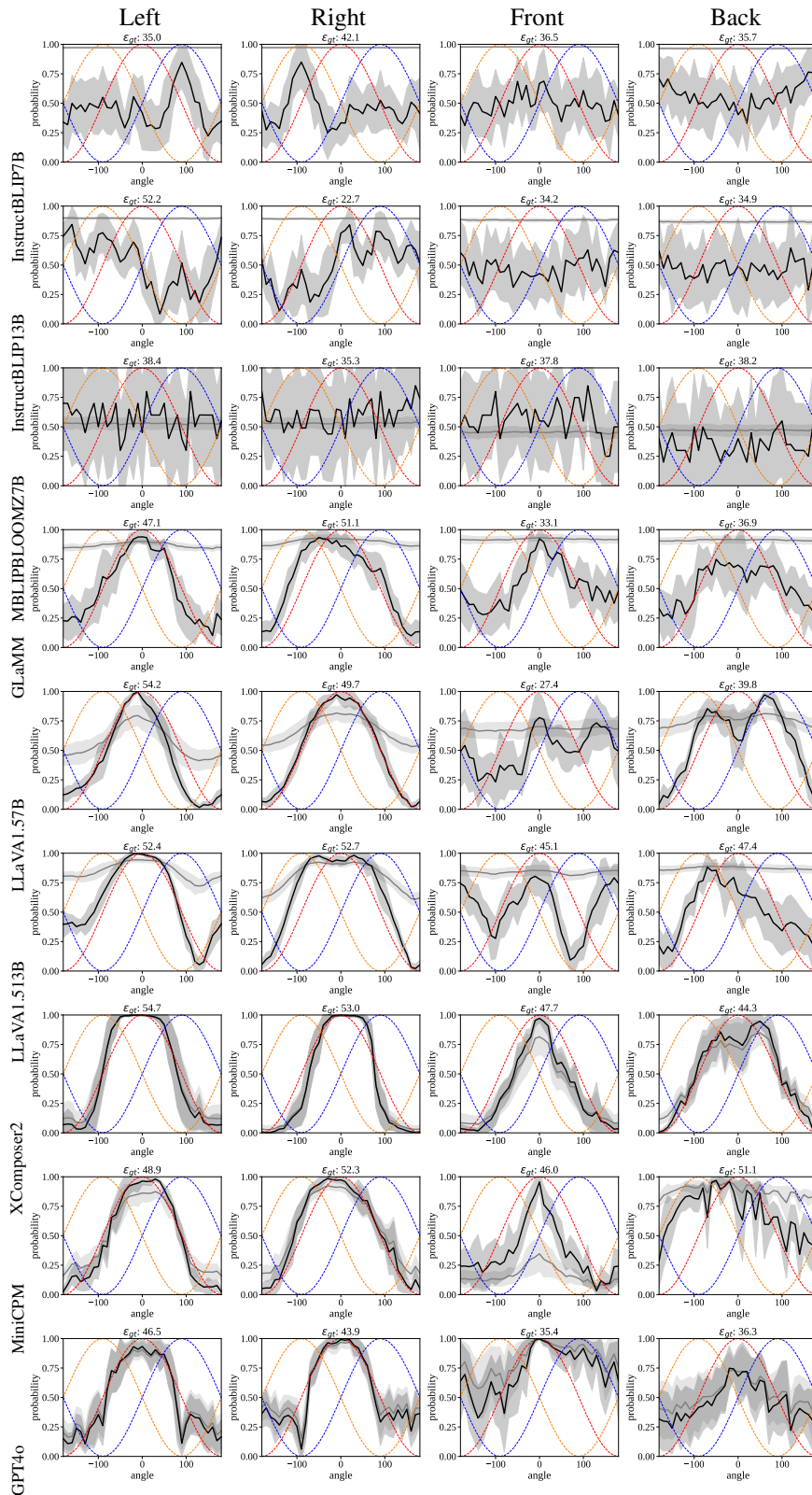
Figure 16: All prediction plots for each model on COMFORT-CAR using the relatum perspective prompt (rel). The raw probability $p(\theta)$ in gray, normalized probability $\widehat{p}(\theta)$ in black, and the reference probabilities $p_{\cos}(\theta)$ of cam in red, add in orange, rel in blue. To avoid overlapping reference probabilities of add and rel, we use plots on COMFORT-CAR with relatum facing left for left and right relations and COMFORT-CAR with relatum facing right for front and behind relations.
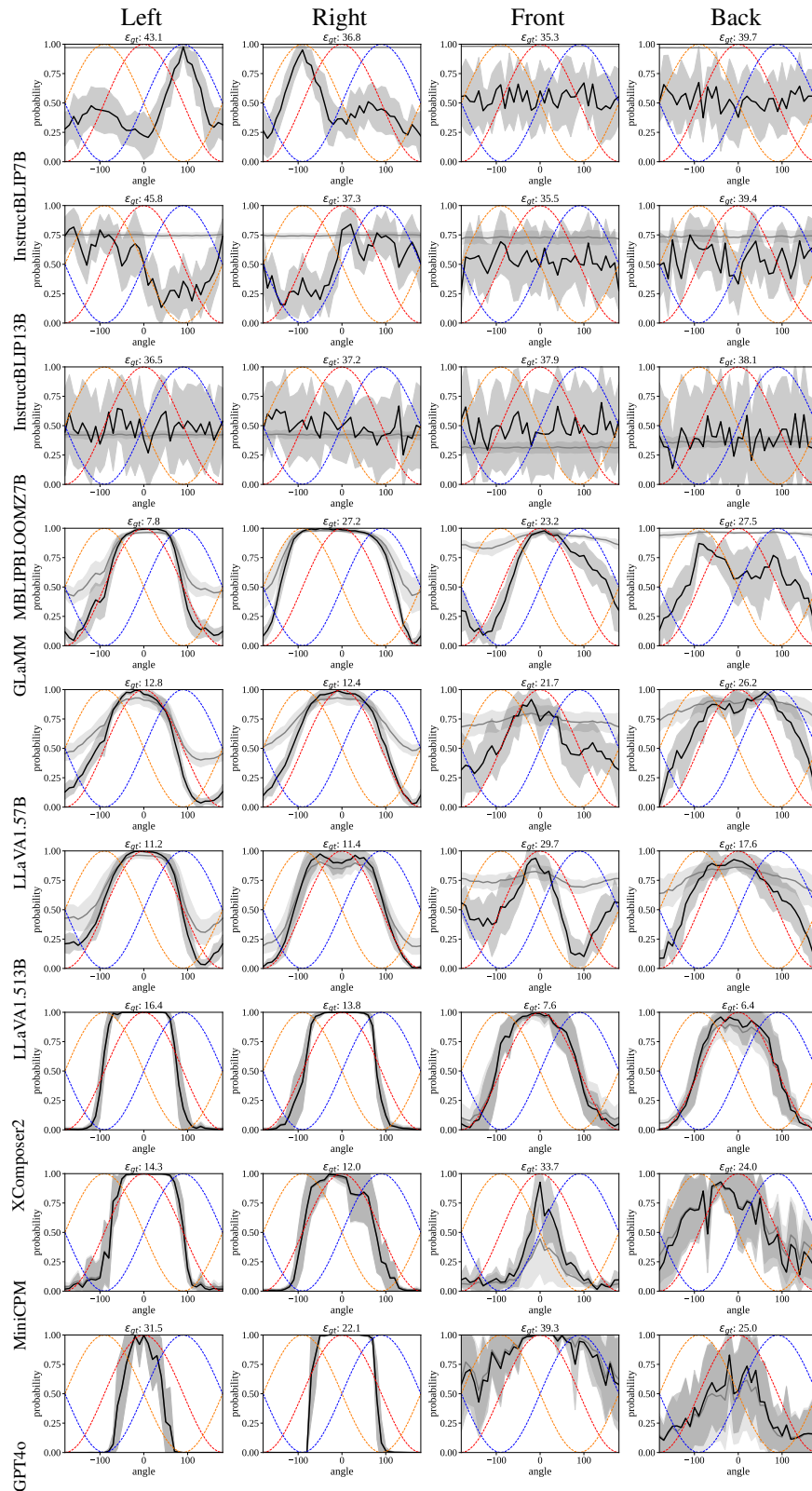
Figure 17: All prediction plots for each model on COMFORT-CAR without perspective prompt (nop). The raw probability $p(\theta)$ in gray, normalized probability $\widehat{p}(\theta)$ in black, and the reference probabilities $p_{\cos}(\theta)$ of cam in red, add in orange, rel in blue. To avoid overlapping reference probabilities of add and rel, we use plots on COMFORT-CAR with relatum facing left for left and right relations and COMFORT-CAR with relatum facing right for front and behind relations.